



Sveriges lantbruksuniversitet
Swedish University of Agricultural Sciences

Department of Forest Genetics
and Plant Physiology

**Analyses of *in vitro* protein-protein interaction of ACT7 or ACT2
and AIP1-2 from *Arabidopsis thaliana* and *in vivo* analysis of AIP1-2
expression**

Jean Claude Nzayisenga

Master thesis, 30 credits • Examensarbete, 30 hp

Master's Program in Plant and Forest Biotechnology, 120 credits

Umeå 2013

SLU, Swedish University of Agricultural Sciences
Faculty of Forest Sciences
Department of Forest Genetics and Plant Physiology

Jean Claude Nzayisenga

Analyses of *in vitro* protein-protein interaction of ACT7 or ACT2 and AIP1-2 from *Arabidopsis thaliana* and *in vivo* analysis of AIP1-2 expression

Analys av *in vitro* protein-protein interaktion av ACT7 eller ACT2 och AIP1-2 från *Arabidopsis thaliana* och *in vivo* analys av AIP1-2 expression

Key words: actin, ACTIN-INTERACTING PROTEIN1-2, *Arabidopsis thaliana*, protein-protein interaction, cell polarity, planar polarity, root epidermis

Supervisor: Markus Grebe, Department of Plant Physiology, Umeå University

Examiner: Erling Ögren, Department of Forest Genetics and Plant Physiology, SLU

Master thesis, 30 credits

Course code: EX0748

Level: A2E

Master's Program in Plant and Forest Biotechnology, 120 credits

Umeå 2013

Table of Contents

1. Summary	1
2. Introduction	3
2.1. Cell polarity	3
2.2. Cell polarity in plants	3
2.3. Planar polarity in multicellular organisms	4
2.4. Planar polarity of root hair positioning in the <i>Arabidopsis</i> root epidermis	5
2.5. <i>ACT2</i> and <i>ACT7</i> in root hair development and planar epidermal polarity in <i>Arabidopsis</i>	7
2.6. Actin dynamics are regulated by actin-binding proteins	8
2.7. AIP1 enhances ADF/cofilin-mediated depolymerization of actin filaments	9
2.8. AIP1 in development and planar polarity establishment of multicellular organisms	11
2.9. <i>AIP1-2</i> genetically interacts with <i>ACT7</i> in <i>Arabidopsis</i>	12
2.10. Cell type-specific enrichment of <i>AIP1-2</i> in the <i>Arabidopsis</i> root epidermis	12
2.11. Aim of this study	13
3. Materials and methods	14
3.1. Materials	14
3.1.1. Laboratory chemicals	14
3.1.2. Culture media	16
3.1.3. Bacteria and <i>Agrobacterium</i> strains	17
3.1.4. Vectors	18
3.1.5. Antibodies	18
3.2. DNA analysis	19
3.2.1. Colony PCR of <i>Agrobacterium</i>	19
3.2.2. Agarose Gel Electrophoresis of PCR products	20
3.3. Transformation	21
3.3.1. Preparation of chemical <i>E. coli</i> competent cells	21
3.3.2. Transformation of <i>E. coli</i>	21
3.3.3. Preparation of <i>Agrobacterium</i> for <i>Arabidopsis</i> transformation	22
3.3.4. Transformation of <i>Arabidopsis</i> with <i>Agrobacterium</i>	22
3.4. Protein analysis	23
3.4.1. Bradford assay	23

3.4.2. Separation of proteins using sodium dodecyl sulfate polyacrylamide gel electrophoresis (SDS-PAGE).....	23
3.4.3. Protein detection on SDS-PAGE gel using Coomassie staining	24
3.4.4. Specific protein detection using Western blot analysis.....	24
3.4.5. Stripping of membranes for additional protein detection.....	26
3.5. Expression and purification of protein from bacteria and extraction of protein from plant.....	26
3.5.1. GST-AIP1-1 and GST-AIP1-2 expression and coupling to the glutathione sepharose beads .	26
3.5.2. Extraction of plant protein for the pull-down experiments	28
3.5.3. Expression of His-ACT2 and His-ACT7 using an IPTG induction system	29
3.5.4. Protein extraction from plants expressing <i>gAIP1-2-Venus</i> or <i>gAIP1-2-mCherry</i>	30
3.6. GST pull-down experiments.....	31
3.6.1. Preparation of glutathione sepharose beads.....	32
3.6.2. <i>In vitro</i> binding assay	33
3.7. Plants growth and materials	33
3.7.1. Plant growth conditions.....	33
3.7.2. BASTA selection of plants after <i>Agrobacterium transformation</i>	34
3.7.3. Crossing T2 plants expressing <i>gAIP1-2-Venus</i> and <i>gAIP1-2-mCherry</i>	34
3.8. Microscope	35
3.8.1. Fluorescence microscopy	35
3.8.2. Light microscopy analysis of root hair positioning	37
4. Results	38
4.1. Analysis of interaction between AIP1-1 or AIP1-2 and actins.....	38
4.1.1. GST-AIP1-1 and GST-AIP1-2 precipitate actins from plant extracts.....	38
4.1.2. His-ACT2 and His-ACT7 expression in Rosetta (DE3) cells.	40
4.1.3. GST-AIP1-2 precipitates His-ACT7 from bacterial protein extracts	42
4.1.4. GST-AIP1-2 precipitates His-ACT2 from bacterial protein extracts	44
4.2. Characterization of <i>AIP1-2</i> overexpressing lines	46
4.2.1. Segregation analysis of fluorescent <i>AIP1-2</i> transgenes.....	46
4.2.2. Expression analysis of fluorescent transgenes using Western blot detection.....	47
4.2.3. Generation of double transgenic lines.	48
4.2.4. Preliminary analysis of root hair-positioning phenotypes of <i>AIP1-2-Venus</i> and <i>AIP1-2-mCherry</i> expressing lines.	50

4.3. Specific <i>AIP-2</i> promoter activity in hair cells	51
4.3.1. Generation of promoter-fusion lines.....	51
4.3.2. Characterization of promoter-fusion lines.....	51
5. Discussion.....	53
5.1. Protein-protein interaction between AIP1 homologs and actins	53
5.1.1. AIP1-1 and AIP1-2 interact with actins from plant extracts	53
5.1.2. His-ACT2 and His-ACT7 expression in Rosetta (DE3) cells.	54
5.1.3. AIP-2 interacts with ACT7.....	55
5.1.4. AIP-2 interacts with ACT2.....	57
5.2. Overexpression of AIP1-2 may lead to an apical shift of root hair positioning.....	58
5.3. <i>AIP1-2</i> appears to be preferentially expressed in hair cell files	59
5.4. Conclusions and perspectives.....	60
6. Acknowledgements.....	62
7. References	63
8. Supplementary figures	70
9. List of abbreviations.....	79

1. Summary

Cell polarity is defined as the polar organization of cellular components along an axis. The coordination of cell polarity within a plane of a single tissue layer is termed planar polarity. An example for planar polarity in plants is the hair formation towards the lower (basal) ends of hair-forming cells in the root epidermis of *Arabidopsis thaliana*. The *ACTIN2* (*ACT2*) and *ACT7* genes are involved in the establishment of planar polarity in the root epidermis. Actin filaments are dynamic structures that undergo a constant turnover including polymerization and depolymerization. In presence of actin-interacting protein 1 (AIP1), depolymerization of actin filaments mediated by actin-depolymerizing factor (ADF/Cofilin) is dramatically increased. In comparison to many other organisms, *Arabidopsis* encodes two *AIP1* copies. *AIP1-1* is expressed in reproductive tissues and *AIP1-2* in all tissues. Despite its conservation throughout eukaryotes, relatively little is known about the developmental roles of AIP1. Here, we investigate the interaction of *Arabidopsis AIP1-2* and actin isoforms and their role during planar polarity.

To this end, we used *in vitro* glutathione-S-transferase (GST) pull-down approaches to study the interactions of AIP1s and actins. These revealed that both recombinant GST-AIP1-1 and GST-AIP1-2 purified from *E. coli* extracts precipitated actins from *Arabidopsis* root cell suspension protein extracts. This indicated that *Arabidopsis* AIP1 homologs are able to interact with actins at the protein level. Furthermore, GST-AIP1-2 precipitated bacterially expressed 6xHistidine (6xHis)-tagged ACT2 (6xHis-ACT2) and 6xHis-ACT7. This strongly suggested that the interaction does not strictly require other plant proteins. Moreover, we generated transgenic lines expressing up to two copies of native AIP1-2, two copies of AIP1-2-Venus and two copies of AIP1-2-mCherry to analyze the effect of AIP1-2 overexpression on root hair positioning. In preliminary analyses, it appeared that root hairs in lines carrying these six copies of *AIP1-2* were shifted more apically than in the wild type indicating *AIP1-2* as a regulator of planar polarity. Transgenic lines expressing an ER-resident mCherry construct under control of the native *AIP1-2* 5' and 3' genomic regions were generated to analyze the *AIP1-2* expression pattern in the root. Highest promoter activity was observed in hair cell files, suggesting that cell file-specific enrichment of AIP1-2 protein did, at least partially, depend on cell file-specific promoter activity. Promoter activity was detected from the elongation zone onwards indicating that *AIP1-2*

transcript is not expressed in the meristem. Taken together, this study shows that *Arabidopsis* AIP1s interact with actins, and that interaction of AIP1-2 with ACT7 and ACT2 does not require other plant proteins *in vitro*. AIP1-2 is transcriptionally upregulated in hair cell files and its overexpression may shift root hair positioning apically, suggesting a regulatory role for AIP1-2 in planar polarity.

2. Introduction

2.1. Cell polarity

Asymmetrical organization of cellular components and structures along an axis known as cell polarity makes one end of the cell to look or behave differently from another (Grebe *et al.*, 2001). The establishment of cell polarity is very crucial for different biological processes of various organisms. In yeast for example, polar cell growth that results in bud formation requires cell polarity (Macara and Mili, 2008). Another example that demonstrates the importance of proper cell polarity establishment in both the animal and plant kingdom is the determination of the main body axis by the polarity of the single-celled zygote. The polarized zygote divides asymmetrically and generates new cells with different fates, ultimately leading to the correct development of organs (Mayer *et al.*, 1993; Ueda and Laux, 2012). Defects in cell polarity interfere with cellular functions and create abnormalities such as misregulated cell divisions, lack of and malformed organs (Mayer *et al.*, 1993). Thus, studying cell polarity can provide key concepts to understand growth and development of unicellular and multicellular organisms.

2.2. Cell polarity in plants

Cell polarity always describes the organization of cellular components relative to a particular axis. The major body axis in plants is the apical-basal axis which delineates the shoot (apical) to root (basal) axis (Mayer *et al.*, 1991). In *Arabidopsis*, the first signs of apical-basal axis formation are already morphologically expressed as zygote polarity during embryogenesis. The starting point of a sexually produced organized organism is the fertilized egg cell called zygote. The zygote of many flowering plant species divides into a smaller apical cell that gives rise to almost the entire embryo and a larger basal cell that will produce the root (Friml *et al.*, 2003; Grebe, 2004). During later stages of embryo development, the polar accumulation of PIN auxin efflux carriers at the plasma membrane can be observed. This polar localization is thought to guide auxin flow and to promote the establishment and maintenance of an auxin gradient necessary for plant growth and development (Fig. 1B). PIN polar localization is commonly used as a model to

investigate cell polarity (Kleine-Vehn and Friml, 2008). Other processes or systems where cell polarity can be observed are the polar tip growth of pollen tubes and of root hairs (Fig. 1A, 1B) (Grebe *et al.*, 2001; Yang, 2008). Using these systems, the establishment and maintenance of cell polarity in plants has been linked to physical factors such as light and gravity. In addition, ion fluxes such as calcium (Ca^{2+}) fluxes, plasma membrane and cytoskeleton along with vesicular trafficking are also involved in cell polarity of plants (Grebe *et al.*, 2001).

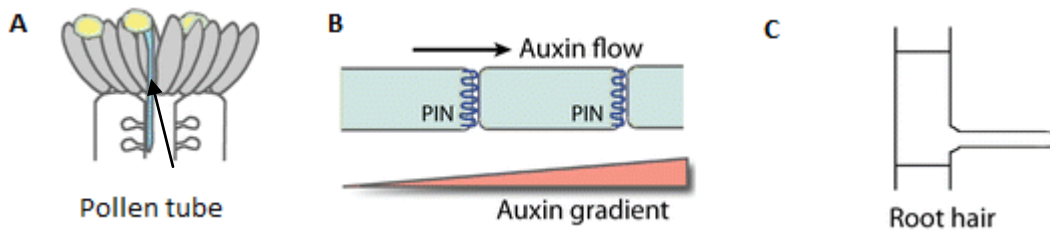


Figure 1. Model systems for studying cell polarity in plants. **A.** Upper part of a pistil showing the pollen tube that is growing. **B.** Polar localization of PIN required for auxin gradient formation. **C.** Cell polarity of root hairs (adapted from Yang, 2008).

2.3. Planar polarity in multicellular organisms

Cell polarity may be coordinated within the plane of a specific tissue layer. This coordination is defined as ‘planar polarity’ (Grebe, 2004). In animals, the proper anatomy and function of different tissues and organ rely on planar polarity (Thomas and Strutt, 2012). A model system to study planar polarity in *Drosophila* is the wing epithelium, a single tissue layer where hairs develop polarly organized along the proximal-distal axis of the wing (Thomas and Strutt, 2012). Hairs are located at the distal side of each cell and are oriented in distal direction (Fig. 2A). In *Arabidopsis*, the emergence of root hairs close to the basal end of hair forming cells in the root epidermis can be used as a model system to study planar polarity (Fig. 2B). There are some parallels between planar polarity of wing hairs in *Drosophila* and of root hairs in *Arabidopsis*. However, the molecular mechanisms underlying planar polarity in plants and animals seem to be quite different. In *Drosophila*, the components of the Frizzled pathway acts upstream to conduct

a planar polarity signal. In *Arabidopsis*, core components of the Frizzled pathway are not present within the genome. Recent findings revealed that in the *Arabidopsis* root, auxin can act as a directional cue via a concentration gradient during establishment of planar polarity (Fischer *et al.*, 2006; Ikeda *et al.*, 2009).

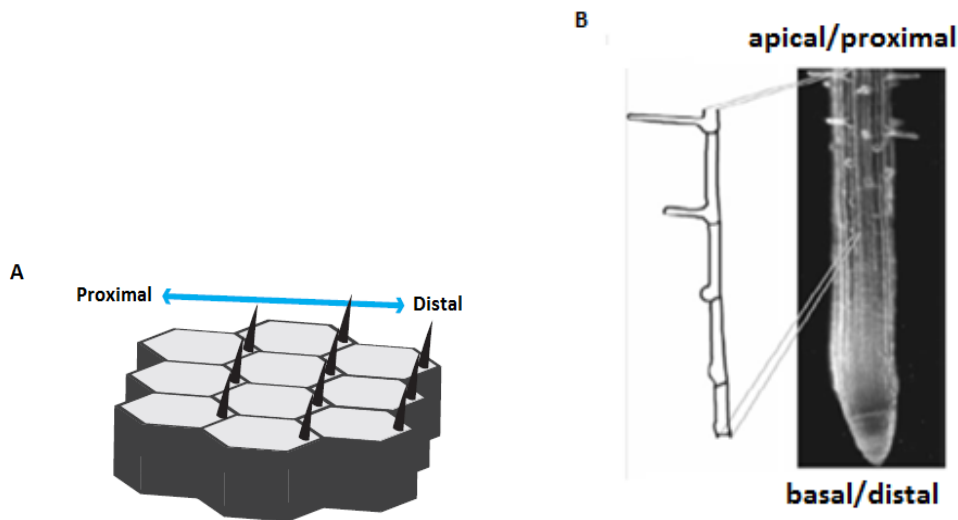


Figure 2. Planar polarity in animals and plants. **A.** Wing hairs in *Drosophila* are placed at distal ends of cells and are oriented towards the distal end of the wing. **B.** Root hair outgrowth towards the basal end of hair forming cells in the epidermal tissue layer of *Arabidopsis* (adapted from Grebe, 2004; Marcinkevicius *et al.*, 2009).

2.4. Planar polarity of root hair positioning in the *Arabidopsis* root epidermis

In *Arabidopsis thaliana*, root hairs are positioned along the outer membrane of root epidermal cells towards their root-tip oriented (basal) end. The root tip is where the auxin gradient reaches its maximum concentration. The view that an auxin gradient can act as a directional cue for polar root hair positioning is supported by the findings that local reconstitution of an auxin gradient in an *aux1;ein2;gnom^{eb}* mutant that lacks a graded auxin distribution in the root polarizes root hair formation towards the source of auxin application (Fischer *et al.*, 2006). The establishment of the endogenous auxin gradient in the root tip requires both local auxin biosynthesis as well as

directional transport of auxin away from its concentration maximum (Ikeda *et al.*, 2009). CTR1 is a negative regulator of ethylene response genes that acts to repress the local expression of two auxin biosynthesis genes in the root tip (Fig. 3A) (Ikeda *et al.*, 2009). *ctr1* mutants show an increase in auxin concentration in the root tip and an increase in the auxin gradient, accompanied by a shift of root hair positioning towards the basal-most ends of cells oriented towards the root tip (Ikeda *et al.*, 2009). The dependence of the auxin gradient on coordinated transport of the plant hormone was observed in *aux1;ein2;gnom^{eb}* mutants that lack an auxin concentration gradient (Fischer *et al.*, 2006). AUX1 is an influx auxin carrier, whereas EIN2 is a positive regulator of ethylene response gene, whose activity can be inhibited by CTR1, and GNOM is required for auxin efflux carrier PIN1 and PIN2 polar localization at the plasma membrane (Marchant *et al.*, 1999; Alonso *et al.*, 1999; Steinmann *et al.*, 1999; Kleine-Vehn *et al.*, 2008; Ikeda *et al.*, 2009). In addition, *aux1;ein2;gnom* mutants display an apical shift of Rho-GTPases of plant (ROP) localization compared to the wild type (Fischer *et al.*, 2006). Taken together, local auxin biosynthesis and directional auxin transport cooperate to generate an auxin concentration gradient necessary for ROP localization at the root hair initiation site (Fig. 3A, 3B). Similar to ROP localization, root hair positioning is shifted apically in *aux1;ein2;gnom^{eb}* mutants (Fischer *et al.*, 2006). It is assumed that ROP determines the root hair initiation site, since ROP2 overexpression results in multiple root hairs emerging from each cell (Fig. 3B) (Jones *et al.*, 2002). However, the components acting downstream of ROPs during the establishment of planar polarity in the *Arabidopsis* root epidermis remain elusive. In different model systems such as *Arabidopsis* pollen tubes or *Drosophila* wing epithelial cells, ROPs have been shown to organize the actin cytoskeleton that could be involved in the symmetry breaking process of the cell (Fig. 3B) (Eaton *et al.*, 1996; Fu and Yang, 2001; Jones *et al.*, 2002; Li and Gundersen, 2008).

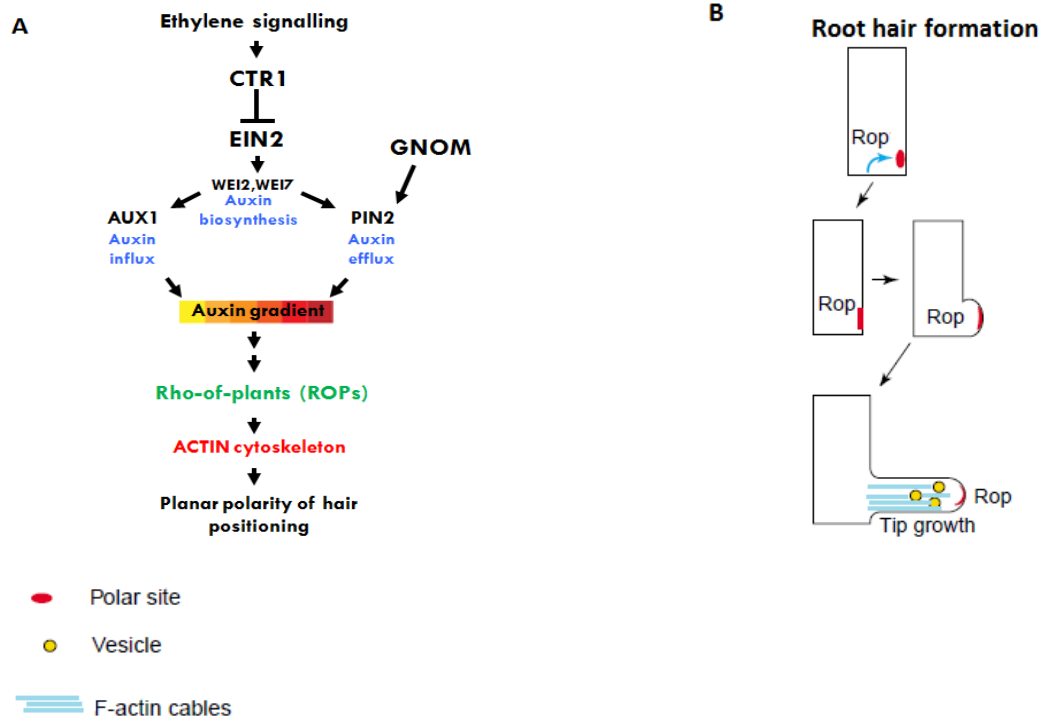


Figure 3. A. Proposed model for establishment of planar polarity of root hair positioning in *Arabidopsis* root epidermis. **B.** Root hair formation in *Arabidopsis*. ROP organizes the actin cytoskeleton at the root hair initiation. Vesicular trafficking associated with actin cytoskeleton is also required for root hair initiation (adapted from Grebe *et al.*, 2002; Fischer *et al.* 2006; Ikeda *et al.*, 2009; Fu and Yang, 2001).

2.5. ACT2 and ACT7 in root hair development and planar epidermal polarity in *Arabidopsis*

Actin as a major component of the cytoskeleton is involved in several biological processes in all eukaryotic cells. These include cell division, cell morphology, organelle transport and cell polarity (Cramer, 2008; Fu and Yang, 2001b; Liu *et al.*, 2011; Pollard and Cooper, 2009). According to phylogenetic studies and expression patterns, *Arabidopsis* encodes eight *ACTIN* (*ACT*) genes that are expressed preferentially in vegetative or reproductive tissues (Fig. 4A). *ACT2* and *ACT7* are expressed preferentially in vegetative tissues and are involved in root hair development (Kandasamy *et al.*, 2009). In root hair-forming cells, root hair development can be grouped into distinct steps involving selection of a polar root hair initiation site, bulge formation

at this site and root hair elongation by tip growth (Dolan *et al.*, 1994). *act2* mutants, in some cases show bulges from a more apical location than the wild type and occasionally two hairs may form from the same cell. In addition, *act2* mutants have much shorter root hairs than the wild type. This suggests that ACT2 participates in selection of the polar hair initiation site and in root hair elongation by tip growth (Ringli *et al.*, 2002). The *act7* mutant displays a decrease in root hair density but the root hair growth is not affected. This suggests that ACT7 is required for early stages of root hair formation rather than for root hair elongation (Kandasamy *et al.*, 2009). Importantly, *act2 act7* double mutants show a considerably stronger apical shift of root hair positioning compared to the wild type and the respective single mutants (Ikeda and Grebe, unpublished results). Taken together, understanding the role of ACT2 and ACT7 during establishment of planar polarity can shed light on the isoform-specific contribution to distinct developmental processes such as polar root hair initiation site selection, bulging and root hair elongation. This may also deepen our understanding of mechanistic details of the regulation of actin dynamics by actin-binding proteins during planar polarity establishment.

2.6. Actin dynamics are regulated by actin-binding proteins

Actin, a 42 kDa globular protein, can polymerize into actin filaments which in turn are able to depolymerize (Moseley and Goode, 2006). In its ATP-bound state, globular (G)-actin can bind to the barbed or plus ends of preexisting actin filaments. The ATP is slowly degraded into ADP and phosphate, a process that facilitates actin filament depolymerization at the pointed end (minus end) (Van der Honing *et al.*, 2007). Polymerization of actin filament is mostly associated with the barbed end whereas depolymerization is mostly associated with the pointed end (Fig. 4B). Actin-binding proteins regulate polymerization and depolymerization of actin to achieve appropriate actin dynamics. Arp2/3 and formin are the major proteins that are involved in actin polymerization. Formin promotes extension of actin filaments at the barbed end, while Arp2/3 mediates formation of branches resulting in branched actin filaments (Lew, 2002; Young *et al.*, 2004). Actin depolymerizing factor (ADF; also called Cofilin, COF) is one of two major depolymerizing factors of actin filaments. ADF can act directly by severing actin filaments or indirectly by increasing the dissociation of G-actin at the pointed end (Fig. 5B) (Ono, 2003). The

activity of ADF is controlled by different cellular mechanisms such as pH and phosphorylation status (Ono, 2003). Interestingly, another actin-binding protein, the actin-interacting protein 1 (AIP1), has been shown to strongly enhance the actin filament severing activity of ADF (Ono, 2003). Despite the knowledge about many of the actin-binding proteins, relatively little is known about their precise mechanistic functions and about their regulation during development. Since actin is required for several fundamental processes, it is crucial to understand its regulation by actin-binding proteins.

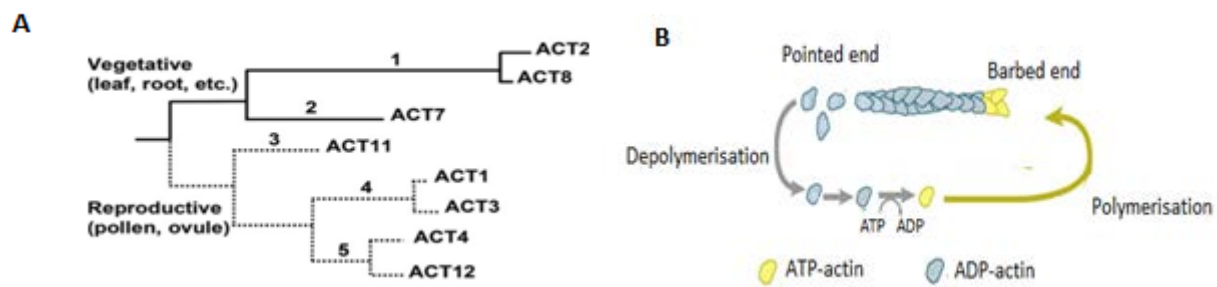


Figure 4. **A.** Phylogenetic tree of the eight actin genes from *Arabidopsis thaliana* integrating their overall expression pattern. **B.** Actin dynamics. Depolymerization is associated with the pointed end containing ADP bound G-actin while polymerization is associated with the barbed end containing ATP bound G-actin (adapted from Alwood *et al.*, 2002; Le Clainche and Carlier, 2008).

2.7. AIP1 enhances ADF/cofilin-mediated depolymerization of actin filaments

Controlled depolymerization of actin filament is crucial for actin dynamics. For example, when a rapid rearrangement of actin filaments is required, depolymerization provides actin monomers for assembly of new actin filaments (Ono, 2003). AIP1 is a 67 kDa WD-repeat protein that enhances the depolymerizing function of ADF towards actin filaments in yeast, animal and plants (Allwood *et al.*, 2002; Mohri and Ono, 2003; Ketelaar *et al.*, 2004; Ren *et al.*, 2007). For all AIP1 homologs known to date, the structure of AIP1 contains around 14 WD-repeats organized in two seven-blade β -propellers (Mohri *et al.*, 2004). WD-repeat proteins are generally known to bind to other proteins and to form multiprotein complex (Hussey, 2004). AIP1 alone slightly depolymerizes actin filaments but it can strongly increase the depolymerizing activity of ADF.

Arabidopsis AIP1-1 for instance has been shown to increase the actin depolymerizing activity of lily ADF *in vitro* about 2.8 fold (Allwood *et al.*, 2002). How AIP1 enhances ADF activity is still not well understood. AIP1 has been shown to cap barbed ends of short actin filaments generated by ADF (Ono, 2003). Thus, AIP1 prevents polymerization at the barbed end and promotes depolymerization at the pointed end (Fig. 5A) (Ono, 2003). This is because in addition to severing activity, ADF is also able to bind to G-actin at the pointed end to accelerate depolymerization (Okada *et al.*, 2002). However, another study using fluorescence microscopy demonstrated that AIP1 directly severs ADF-bound actin filaments (Ono *et al.*, 2004). This suggests that AIP1 increases ADF polymerization by severing ADF-decorated actin filaments (Fig. 5B) (Ono *et al.*, 2004). Considering the importance of a tight control of actin dynamics and the requirement for AIP1 in this process, deepening our understanding of the underlying molecular mechanisms might help to understand the precise physiological function of AIP1.

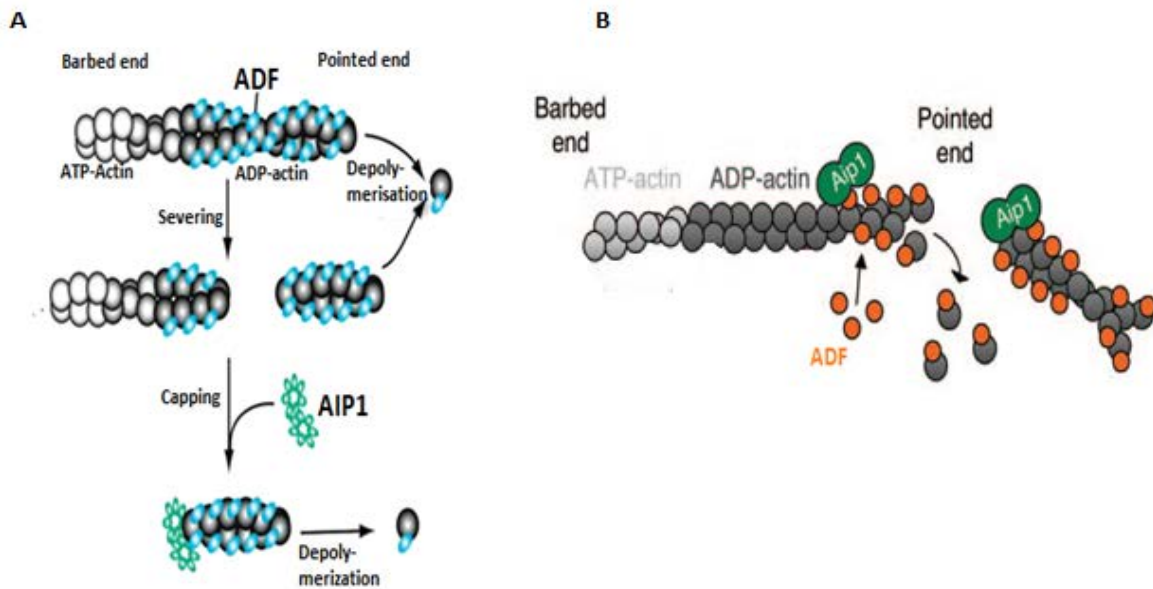


Figure 5. **A.** AIP1 enhances actin filament disassembly by capping the barbed end. **B.** AIP1 enhances actin filament disassembly by participating in severing of ADF bound actin filament (adapted from Ono, 2003; Moseley and Goode, 2006).

2.8. AIP1 in development and planar polarity establishment of multicellular organisms

Because AIP1 is involved in regulation of actin, several actin-based functions are impaired by absence or by partial reduction of AIP1 function. Whereas *aip1* single mutants in budding yeast do not show a strong growth defect, a striking role of AIP1 in yeast is revealed by the strong synergistic genetic interaction between yeast *AIP1* and the gene encoding ADF, *COF1* (Iida and Yahara, 1999; Rodal *et al.*, 1999). In addition to defects in cell proliferation, planar polarity of wing epidermal hairs is compromised in *Drosophila flare* (*flr*) mutants, defective in the fly *AIP1* homolog, as well as in *twinstar* (*tsr*) mutants defective in the fly *ADF/COF* homologue which both produce multiple hairs and hairs with defective orientation from single cells (Blair *et al.*, 2006; Ren *et al.*, 2007). Consistent with a suggested role for AIP1 in actin filament disassembly, *Drosophila flr* mutants show a higher amount of actin filaments compared to the wild type (Ren *et al.*, 2007). In *Physcomitrella patens*, deletion of *AIP1* interferes with polar cell growth. In addition, severing frequency is decreased and actin filaments bundles (actin cables) are increased indicating the role of AIP1 for actin filament disassembly in this moss (Augustine *et al.*, 2011). The *Arabidopsis* genome harbors two *AIP1* genes; *AIP1-1* is expressed mainly in reproductive tissues and *AIP1-2* in both vegetative and reproductive tissues (Allwood *et al.*, 2002). Reduction of both *AIP1-1* and *AIP1-2* expression by RNA interference decreases the growth of roots, leaves and flowers and plants are not viable in most severe cases. *AIP1* RNAi lines show short root hairs and ectopic localization of actin cables in root tip cells, whereas lines ectopically overexpressing *AIP1-1* have a defect in actin organization and display short root hairs that are thick and swollen (Ketelaar *et al.*, 2004; Ketelaar *et al.*, 2007). So far, no single-mutant phenotype for any of the two *Arabidopsis AIP1* homologs has been published. However, Markus Grebe's laboratory has observed a function for *AIP1-2* in the establishment of planar polarity. In *aip1-2* mutants, root hairs are positioned more to the basal ends of root hair-forming cells compared to the wild type (Claes, Kiefer and Grebe, unpublished results). To further examine whether *AIP1-2* may act as a regulator of polar positioning of root hairs, it will be interesting to further analyze planar polarity phenotypes of *AIP1-2* overexpressing plants.

2.9. *AIP1-2* genetically interacts with *ACT7* in *Arabidopsis*

The first AIP1 homolog described was budding yeast Aip1p that was identified as an actin-binding protein using a yeast two-hybrid screen for actin-interacting proteins (Amberg *et al.*, 1995). Similarly, in a screen for interactors of *Arabidopsis* ACT7, the *Arabidopsis* homolog AIP1-2 was identified as a potential interactor (Ikeda and Grebe, unpublished results). After confirming this interaction in the yeast two-hybrid system (Claes, Kiefer and Grebe, unpublished results), Markus Grebe's group observed that *aip1-2;act7* double mutants display a very strongly reduced germination rate compared to the single mutants, indicating a synergistic genetic interaction of the *ACT7* and the *AIP1-2* genes *in vivo* (Kiefer and Grebe, unpublished results).

2.10. Cell type-specific enrichment of AIP1-2 in the *Arabidopsis* root epidermis

The *Arabidopsis* root epidermis is patterned into hair cell files and non-hair cell files. The designation of root hair cell fate in *Arabidopsis* depends on the position of the epidermal cell relative to the underlying cortical cell. Epidermal cells that originate from a position overlying two cortical cells become a hair cell (trichoblast) and epidermal cells that originate from over just one cortical cell become a non-hair cell (atrichoblast) (Lin and Aoyama, 2012). Hair cells differ from non-hair cells even before hair formation by different characteristics such as higher cell division rates and shorter cell length (Berger *et al.*, 1998; Dolan and Costa, 2001). In addition, the gene expression program differs between hair and non-hair cell files. For example, *GLABRA2* (*GL2*) which is necessary for designation of non-hair cell fate is expressed only in non-hair cell files (Lin and Aoyama, 2012). Interestingly, functional AIP1-2-mCherry protein expressed under the control of the *AIP1-2* genomic region is preferentially expressed in hair cells from early cell elongation onwards (Kiefer and Grebe, unpublished results). It is, therefore, interesting to further examine the promoter activity of the *AIP1-2* gene.

2.11. Aim of this study

The first aim of this study was to further analyze the interaction primarily of AIP1-2, but also of AIP1-1, with *Arabidopsis* actins using a biochemical assay. To this end, glutathione-S-transferase (GST) pull-down assays were planned to analyze protein-protein interaction *in vitro*. In order to perform GST-pull down assays, GST-AIP1-2 and GST-AIP1-1 were planned to be expressed in and purified from *E. coli* to pull down actin from *Arabidopsis* protein extracts. The second aim was to test whether AIP1-2 can interact with recombinant ACT2 and ACT7 *in vitro*. To investigate this, GST-AIP1-2 was chosen to attempt to perform pull-down assays of 6xHistidine (6xHis)-tagged-ACT7 (6xHis-ACT7) or 6xHis-ACT2 from *Arabidopsis* expressed in and purified from *E. coli*. In the yeast two-hybrid system, interaction between *Arabidopsis* actins and AIP1s could theoretically be mediated by yeast ADF/Cof1p, whereas pulling down either purified 6xHis-ACT2 or 6xHis-ACT7, or the same proteins contained in bacterial protein extracts, would eliminate this possibility, because bacteria do not encode ADF-like proteins. Given that *aip1-2* mutants display a basal shift of root hair positioning, the third aim of the study was to examine whether AIP1-2 modulates polar root hair positioning in a dosage-dependent manner. Plants overexpressing additional functional copies of AIP1-2 were to be generated and examined for the expression profile of the fluorescently tagged AIP1-2 transgenes using confocal laser scanning microscopy. After initial expression analysis of AIP1-2 overexpressing lines, seedlings were planned to be phenotypically analyzed, for example for root hair positioning defects, by light microscopy. The fourth and last aim of this study was to start to attempt to understand the mechanism of cell file-specific AIP1-2 enrichment. To initially address this question, an endoplasmic reticulum (ER)-resident mCherry construct under control of the AIP1-2 promoter was planned to be transformed into the wild type of *Arabidopsis thaliana* and T2 seedlings were planned to be analyzed for AIP1-2 promoter activity in the root by confocal laser scanning microscopy.

3. Materials and methods

3.1. Materials

3.1.1. Laboratory chemicals

Laboratory chemicals for this study were supplied by different companies including Sigma Aldrich (Sigma-Aldrich Sweden AB, Stockholm, Sweden), Bio-Rad (Bio-Rad Laboratories AB, Sundbyberg, Sweden), Duchefa (Haarlem, Netherlands), Roche (Mannheim, Germany), Invitrogen (Invitrogen Ltd., European Headquarters, Paisley, UK) and Merck (Darmstadt Germany).

Table 1: Buffers and Solutions

Method	Buffer/solution	Components
Preparation of chemical competent cells	TFBI buffer	30 mM potassium acetate, 100 mM RbCl ₂ , 10 mM CaCl ₂ , 50 mM MnCl ₂ ; 15% (v/v) glycerol, pH 5.8 with glacial acetic acid
	TFBII buffer	10 mM NaMOPS, 75 mM CaCl ₂ , 10 mM RbCl, 15% v/v glycerol
Bacterial protein extraction	Buffer A	1 mM EDTA, 5 mM DTT, 1 mM ADP, 0.1 mM PMSF, 2 mM DIFP, 10 mM Tris HCl, pH 8.0
Plant protein extraction	Extraction buffer	25 mM Tris pH 7.5, 10 mM MgCl ₂ , 2 mM DTT, 100 mM NaCl, 0.2% Tween, 10% glycerol, 5 mM EGTA
GST-pull-down experiments	PBS buffer	140 mM NaCl, 2.7 mM KCl, 10 mM Na ₂ HPO ₄ , 1.8 mM KH ₂ PO ₄ , pH 7.3
	Bead-binding buffer	140 mM K ₃ PO ₄ , 150 mM KCl, 1mM MgCl ₂ , pH 7.5

SDS-PAGE	Resolving gel	2.1 ml H ₂ O , 4.0 ml 30% acrylamide mix (Bio-Rad), 3.75 ml 1M Tris-HCl pH 8.8, 100 µl 10% SDS, 65 µl 10% APS , 6 µl TEMED
	Stacking gel	2.75 ml H ₂ O , 666 µl 30% acrylamide mix (Bio-Rad), 500 µl 1M Tris-HCl pH 6.8, 50 µl 10%
	SDS buffer	SDS, 30 µl 10% APS , 5 µl TEMED, 25 mM Tris base, 0.1% SDS, 200 mM Glycine
	5x SDS loading buffer	6 ml 1 M Tris-HCl pH 6,8, 10 ml glycerol, 1 ml β-mercaptoethanol, 2 g SDS, 1 ml 1%, Bromophenol blue
Western blot	Transfer buffer	75 ml Tris-HCl pH 7.6, 150 ml 0.5 M boric acid, 1275 ml distilled water.
	TBST	250 mM Tris-HCl, 750 mM NaCl, 0.1% Tween- 20, pH 8.0
	TBS	250 mM Tris-HCl, 750 mM NaCl, pH 8.0
	Stripping buffer	20 ml 10% SDS, 6.25 ml 1 M Tris-HCl, 73,75 ml distilled water, 0.8 ml β-mercaptoethanol
Coomassie staining	Staining solution	0.1% Coomassie blue R-250, 40% Ethanol, 10% acetic acid
	Destaining solution	40% ethanol, 10% acetic acid, 5% glycerol
Gel electrophoresis	TAE buffer composition	4.84 g/l Tris, 0.114% glacial acetic acid, 0.742 g/l Na ₂ EDTA.2H ₂ O, pH 8.0
	5x Orange G loading buffer	20 mg Orange G, 6 ml glycerol, 1.2 ml 0.5 M EDTA, 2.8 ml dH ₂ O
Seed sterilization	Sterilization solution	70% (v/v) ethanol, 0.05% (v/v) Triton X-100
	10x Bayrochlor solution	1 Bayrochlor tablet (3 g), 27 ml dH ₂ O

Root hair positioning	Clearing solution	chloralhydrate:glycerol:H ₂ O (8:3:1)
	Ethanol Clearing solution	chloralhydrate:glycerol:H ₂ O (8:3:1), 70% ethanol

3.1.2. Culture media

Media used to grow *Escherichia coli*, *Agrobacterium tumefaciens* and *Arabidopsis thaliana* are indicated in Tab. 2. For *Arabidopsis* suspension cultures using MSAR medium, the culture was subcultured every week by inoculating 10-15 ml culture into new 100 ml MSAR medium.

Table 2: Culture media

Species	Medium	Components
<i>E. coli</i> and <i>Agrobacterium</i>	LB	10 g/l Bacto-Tryptone, 5 g/l Bacto-Yeast extract, 5 g/l NaCl
	LB agar	10 g/l Bacto-Tryptone, 5 g/l Bacto-Yeast extract, 5 g/l NaCl, 15 g/l Bacto-Agar
<i>E. coli</i>	Auto induction medium	928 ml ZY medium (1% N-Z-amine, 0.5% yeast extract), 1 ml 50x medium (50 mM FeCl ₃ x6H ₂ O , 20mM CaCl ₂ x2H ₂ O, 10 mM MnCl ₂ x 4H ₂ O, ZnSO ₄ 7xH ₂ O, 2 mM CoCl ₂ x 6H ₂ O, 2 mM CuCl ₂ x 2H ₂ O, 2mM NiCl ₂ x 6H ₂ O, 2 mM Na ₂ MoO ₄ x 2H ₂ O, 2mM H ₃ BO ₃), 20 ml 50x5052 medium (25% glycerol, 2.5% glucose, 10% lactose)

<i>A. thaliana</i>	MS medium	4.3 g MS salt, 10 g sucrose, 0.5 g MES, pH 5.8 with KOH
	MS agar medium	4.3 g MS salt, 10 g sucrose, 0.5 g MES, 8 g PhytoAgar, pH 5.8 with KOH
	MSAR medium	4.33 MS basal salts, 2 ml 100x B5 vitamin (200 mg/l Myo-inositol, 1 mg/l Nicotinic acid, 1 mg/l Pyridoxine HCl, 10 mg/l Thiamine HCl), 30 g sucrose (3 %), 0.24 mg/l 2,4-D, 0.014 mg/l kinetin, pH 5.7 with KOH

3.1.3. Bacteria and *Agrobacterium* strains

Bacteria and *Agrobacterium* strains use are indicated in Tab.3.

Table 3: Bacteria and *Agrobacterium* strains

Species	Strain	Genotype	Selectable marker
<i>Escherichia coli</i>	Rosetta (DE3)	F ⁻ ompT hsdS _B (r _B ⁻ m _B ⁻) gal dcm (DE3) pRARE2 (Cam ^R)	Chloramphenicol resistance gene
<i>Agrobacterium tumefaciens</i>	GV3101	T-DNA ⁻ vir ⁺ Rif ^r pMP90 Gent ^r	Gentamycin and rifampicin resistance gene

3.1.4. Vectors

Vectors used for transformation of *Escherichia coli*, *Agrobacterium tumefaciens* are shown in Tab. 4.

Table 4: Vectors

Vector	Company	Selectable marker	Transformed species
pet-GST_1b	EMBL GS	Kanamycin resistance gene	<i>E. coli</i>
pCold I	TAKARA	Carbenicillin resistance gene	<i>E. coli</i>
pGreenII 0229	PGreen	Kanamycin resistance gene	<i>Agrobacterium</i>

3.1.5. Antibodies

Antibodies employed are listed in Tab. 5. All antibodies used were diluted in 2 ml TBST (Tab. 1) containing 2.5% low-fat milk.

Table 5: Antibodies used with their dilutions indicated in brackets.

Antibody	Company	Secondary antibody	Company
mouse anti-actin-11 (1:1000)	Agrisera	anti -mouse (1:10000)	Bio-Rad
mouse anti -GST-HRP (1:1000)	GE Healthcare	-	-
mouse anti -GFP (1:5000)	Covance	anti -mouse (1:10000)	Bio-Rad
rabbit anti -RFP (1:5000)	MBL	anti -rabbit (1:1000)	GE Healthcare
mouse anti -6xHis (1:6000)	Roche	anti -mouse (1:10000)	Bio-Rad

3.2. DNA analysis

3.2.1. Colony PCR of *Agrobacterium*

PCR allows amplification of a specific DNA sequence using forward and reverse primers that specifically recognize the beginning and the end of the sequence to be amplified (Apte and Daniel, 2009). A PCR reaction contains three main steps that are repeated to increase the amount of a specific DNA sequence to be generated. First, at 95 °C, the two complementary strands of DNA are separated, then the temperature is reduced to allow primers to anneal to the complementary regions on the respective strands, and finally the DNA polymerase elongates a new strand by adding nucleotides to primers (Apte and Daniel, 2009).

Prior to this study, the pGreenII vector carrying the ER-resident mCherry construct under control of the native AIP1-2 5' and 3' genomic regions construct had been transformed into *Agrobacterium* (Kiefer, unpublished results). To confirm the presence of the construct in the transformed *Agrobacterium*, a colony PCR was performed. Purified pGreenII vector carrying the construct was used as a control. PCR reaction mix was prepared by adding components in the following order: 5.4 µl distilled water, 0.8 µl dNTPs (4 mM each), 0.8 µl forward primer (10 mM) (Tab. 7), 0.8 µl reverse primer (10 mM) (Tab. 7), 1 µl 10x PCR buffer ammonium sulphate (200 mM), 1 µl MgCl₂ (25 mM) and 0.2 µl (5U/µl) Taq Polymerase (New England Biolabs, Inc.). Finally, the DNA template for the reaction was added by touching an *Agrobacterium* colony and transferring the colony into the PCR reaction vessel. PCR reaction was then performed as indicated in Tab. 6.

Table 6: Reagents of colony PCR reaction

Number of cycles	Time	Temperature
1	2 min	95 °C
30	30 s (denaturation)	95 °C
	30 s (annealing)	55 °C
	1 min (elongation)	72 °C
1	7 min	72 °C
	8 min	10 °C

Table 7: Primers used for colony PCR reaction

Name	Sequence
mChERfXbaI	GCTTTCTAGATGATGAAGACTAATCTTTTTCTCTTTCTCATCTTTTCACTTCTCCTATCAT TATCCTCGGCCGAATTCGTGAGCAAGGGCGAGGAG
mChERrXbaI	GCTTTCTAGAGCGGCCGCAAGCTTCTAAAGTCATCATGCTTGTACAGCTCGTCCATGC

3.2.2. Agarose Gel Electrophoresis of PCR products

Agarose gel electrophoresis is a method to separate DNA fragments based on their size (Sambrook and Russell, 2006). The principle of gel electrophoresis is that DNA is charged negatively due to its phosphate groups and thus migrates towards the positive electrode within an electric field. By passing through an agarose matrix, DNA fragments are separated based on the size where small fragments move faster than larger fragments (Sambrook and Russell, 2006).

To separate DNA fragments amplified by PCR as described above (see 3.2.1.), gel electrophoresis was performed. The mixture of 1% agarose gel and TAE buffer (Tab. 1) was melted and Gel Red™ nucleic acid gel stain was added to the final concentration of 1x before pouring the gel in gel trays containing comb. After gel solidification, TAE buffer was added to completely cover the gel and the comb was removed. The PCR products were mixed with 5x Orange G (Tab. 1) and were loaded into the wells. The DNA ladder (1 kb Plus DNA ladder, Thermo Scientific) was loaded next to the samples. The samples were separated over a gel by applying an electric field with a voltage of 120 V until the dye of the samples reached the end of the gel. Images of fluorescing DNA fragments due to the Gel Red that intercalated with DNA, were taken under ultraviolet light excitation using a Bio-Rad Fluorescent ruler (GelDocXR) instrument.

3.3. Transformation

3.3.1. Preparation of chemical *E. coli* competent cells

E. coli cells were made competent to facilitate the uptake of the vector carrying a DNA fragment of interest during transformation. 4 ml LB medium were inoculated with a single colony (Tab. 2) and the culture was incubated 16 h at 37 °C under agitation at 210 rpm. Two milliliters of saturated culture were inoculated in 100 ml LB and the culture was incubated at 37 °C shaking with 120 rpm until an optical density of 0.5 to 0.6 was reached at a wavelength of 600 nm (OD₆₀₀). The culture was cooled down on ice for 10 min and cells were harvested by centrifugation at 2500 g for 10 min at 4 °C. The pellet was resuspended in 30 ml ice-cold, filter-sterilized TFB I buffer (Tab. 1) and the cell suspension was incubated on ice for 1 h. Cells were collected at 2500 g for 10 min at 4 °C and the pellet was resuspended in 4 ml ice-cold, filter-sterilized TFB II buffer (Tab. 1). The cell suspension was aliquoted in 100 µl, shock-frozen in liquid nitrogen and then stored at - 80 °C.

3.3.2. Transformation of *E. coli*

We transformed vectors carrying an insert of interest into *E. coli*. To this end, 50 µl *E. coli* cells were thawed on ice for 15 min and then mixed with 1 µl (200-300 ng) of the vector. After incubation on ice for 20 min, cells were heat-shocked at 42 °C for 90 s and cooled down on ice for 2 min. Cells were kept at room temperature for 5 min and 250 ml of LB medium was added. The cell suspension was incubated for 1 h at 37 °C under agitation at 230 rpm. Cells were then grown for 16 h at 37 °C under agitation at 230 rpm in LB agar medium containing appropriate antibiotics based on the selectable marker of *E. coli* (Tab. 3), the desired plasmid vector (Tab. 4) and the correct antibiotics concentration (Tab. 3, 4).

3.3.3. Preparation of *Agrobacterium* for *Arabidopsis* transformation

An *Agrobacterium* colony that had been analyzed using colony PCR as described above (see 3.2.1) was inoculated in 5 ml of LB medium containing appropriate antibiotics (Tab. 3, 4) with the proper antibiotic concentration (Tab. 5). The 5 ml culture was incubated for 24 h at 28 °C shaking at 180 rpm. After, the culture had been transferred into 45 ml of LB containing the same antibiotics, the 50 ml culture was grown for 16 h at 28 °C shaking at 180 rpm. The 50 ml culture was transferred to 450 ml of LB containing the same antibiotics and the 500 ml culture was grown for around 6 h at 28 °C at 180 rpm agitation until an OD₆₀₀ of 0.6-0.8 was reached. The cells were then harvested by centrifugation for 20 min at 5000 g and the pellet was resuspended in 5% sucrose solution. Silwet L-77 was added to a final concentration of 0.02% just prior to transformation to increase the accessibility of the plant tissue to the *Agrobacterium*.

3.3.4. Transformation of *Arabidopsis* with *Agrobacterium*

An ER-resident mCherry construct under control of the native AIP1-2 genomic region was transformed into *Arabidopsis thaliana* ecotype Columbia-0 by *Agrobacterium*-mediated transformation. Four-week-old plants with floral buds that were about to open were used for transformation. The above ground parts of plants were dipped twice into bacteria suspension for 5-10 s. After dipping, each plant was covered with a transparent plastic bag and left in the dark for 24 h. The plants were placed in long-day growth conditions as described below (see 3.7.1.) until they produced seeds.

3.4. Protein analysis

3.4.1. Bradford assay

To determine protein concentration in samples, a Bradford assay was performed. The Bradford assay relies on that the red form of Coomassie Brilliant Blue G-250 dye in acidic condition converts into the blue form when it binds to protein leading to an increase in absorbance of the sample (Harlow and Lane, 2006). The absorbance correlates with the protein concentration in the sample and is determined by comparison to a standard curve generated from samples with defined protein concentrations (Harlow and Lane, 2006).

To generate a standard curve, the solution of 0.1 mg/ml bovine serum albumin (BSA) was prepared and 0, 20, 40, 60, 80 and 100 μ l of this solution were added into cuvettes. The cuvettes were complemented with distilled water to reach a volume of 100 μ l per cuvette. For the sample with unknown protein concentration, 2 μ l and 5 μ l were added in duplicate cuvettes. Each sample was mixed with 1 ml of Bradford reagent and left to incubate 5 min prior to measurement. 100 μ l distilled water in the cuvette was used as the negative control (blank) and the absorbance was measured at 595 nm.

3.4.2. Separation of proteins using sodium dodecyl sulfate polyacrylamide gel electrophoresis (SDS-PAGE).

SDS-PAGE is a method to separate proteins based on their molecular weight. Proteins are mixed with the SDS loading buffer, heated at 95 °C for 5 min and cooled down on ice before being applied to the SDS gel (Sambrook and Russell, 2006). SDS is an anionic detergent present in the loading buffer. When the sample is heated, SDS denatures proteins and coats them negatively so that all proteins have approximately the same charge to mass ratio (Sambrook and Russell, 2006). In the presence of an electric field, the negatively charged proteins move towards the positive electrode by passing through a polyacrylamide matrix, where small proteins move faster than larger proteins (Sambrook and Russell, 2006).

After assembling the gel electrophoresis unit, the resolving gel (Tab. 1) was added and 250 μ l of isopropanol was applied on the top to ensure that the top border became even. The gel was left to polymerize for 30-45 min and the isopropanol was subsequently removed using a filter paper. The stacking gel (Tab. 1) was added on the top of the resolving gel and the comb was placed into the stacking gel. The gel was left for 30-45 min to polymerize, placed in tank and SDS buffer (Tab. 1) was added to fill the tank. Proteins were mixed with the SDS loading buffer (Tab. 1), heated at 95 °C for 5 min and cooled down on ice. After removing the comb, 10-15 μ l of each sample were loaded into the wells of the SDS gel and 3 μ l Precision Plus Protein™ Kaleidoscope™ (Bio-Rad) were loaded next to the samples. The samples were separated over the gel by applying an electric field with a voltage of 120 V until the loading dye reached the bottom of the gel.

3.4.3. Protein detection on SDS-PAGE gel using Coomassie staining

The staining of proteins separated over an SDS-PAGE gel was performed using Coomassie staining. The principle of Coomassie staining is that the Coomassie brilliant blue G-250 dye present in Coomassie staining solution in the blue form, is able to bind proteins and to form a complex that can be visualized (Simpson, 2007).

The gel was placed in an adequately sized tank and staining solution (Tab. 1) was added until the gel was covered. The tray containing the gel was then incubated for 2 h at room temperature shaking at around 50 rpm. The staining solution was removed and Coomassie destaining solution (Tab. 1) was added for 2 h to remove unspecifically bound dye that was only loosely attached to the gel and thus to visualize protein bands separated by the gel. The destaining solution was changed 2-3 times during destaining and the images of the gel were acquired.

3.4.4. Specific protein detection using Western blot analysis.

Western blotting is a method used to detect a specific protein after immobilizing on a membrane proteins separated by SDS-PAGE (Sambrook and Russell, 2006). The principle of a Western blot is based on the specific binding of antibodies to the proteins of interest. Since the primary antibodies usually are not linked to a protein that can be used for detection, a secondary antibody

is used to detect the primary antibody (Sambrook and Russell, 2006). The secondary antibody which is able to bind to the primary antibody, is conjugated with a probe to indirectly detect the protein. The commonly used probe is horseradish peroxidase (HRP) which cleaves its substrate, luminol, leading to fluorescence. The fluorescence intensity corresponds to the amount of protein (Sambrook and Russell, 2006).

To transfer the proteins separated via SDS gel electrophoresis as described above (see 3.4.2.) to a Polyvinylidene Fluoride (PVDF) membrane (Sigma) that can be used for Western blotting, the gel was placed facing a PVDF membrane that had been immersed in 100% methanol for 15 s to promote humidification of the membrane. The membrane was then washed 3x in distilled water and left to equilibrate in transfer buffer (Tab. 1) around 5 min before transfer. Sponge, filter papers and gel were also equilibrated in transfer buffer around 5 min before transfer. A Western blot sandwich was arranged from the black side (which was oriented towards the negative pole) to the white side (which was oriented towards the positive pole) of the cassette as follows: sponge, whatman filter paper, gel, membrane, whatman filter paper and sponge. The hydrophobic side of the membrane which is originally tightly attached to a protective paper was facing the gel in the assembly. The assembly was placed into the holder and put in the tank filled with transfer buffer. The stirring bar was put inside the tank to keep homogeneous conductivity and temperature during the transfer. The protein transfer was performed at 20 V constant for 1 h followed by 45 min at 25 V. The membrane was removed from the assembly cassette and rinsed in distilled water and briefly in TBST (Tab. 1). The protein side was always up during rinsing or washing. The membrane was blocked in TBST containing 5% low-fat milk for 2 h under agitation at around 50 rpm at 22 °C or overnight at 4 °C to prevent unspecific antibody binding to the membrane. The membrane was rinsed in TBST and incubated with the primary antibody in 50 ml Falcon tube rotating for 2 h at 22 °C. The membrane was washed 3x in TBST for 10 min. Subsequently, the membrane was incubated with secondary antibody under the same conditions applied for the primary antibody but for only 1 h. The membrane was washed 3x in TBST and 1x in TBS (Tab. 1) for 10 min per wash. After placing the membrane between two plastic sheets, Amersham ECL™ reagent (GE Healthcare) was used as described by the manufacturer and the fluorometric reaction recorded by taking pictures using a charge-coupled device (CCD) camera (Fujifilm) or film developer. To develop the membrane with film, the membrane was placed into the film cassette and the film was exposed to the membrane in the dark room for a specific time.

The film was then placed in a developer machine (AGFA Gevaert) containing developing solutions (AGFA Gevaert). After analysis, the membrane was washed in TBST for 10 min and stored at 4 °C to be stripped later and reprobed.

3.4.5. Stripping of membranes for additional protein detection

After Western-blot analysis as described above (see 3.4.4), the membrane was stripped to detect other proteins. Twenty milliliters of stripping buffer (Tab. 1) was added in a 50 ml falcon and warmed at 50 °C. The membrane was then placed into the 50 ml falcon tube and incubated at 50 °C for 45 min on a rotating wheel. After, the membrane was washed for 2 hr with distilled water and each 10 min the distilled water was changed and finally washed 5 min with TBST. At this step, the membrane was ready for blocking stage in TBST containing 5% low-fat milk powder as described above (see 3.4.4). Pictures were acquired using CCD camera and films as described above (see 3.4.4). The membrane was then washed with TBS for 10 min and stored at 4 °C for further reprobing if necessary.

3.5. Expression and purification of protein from bacteria and extraction of protein from plant

3.5.1. GST-AIP1-1 and GST-AIP1-2 expression and coupling to the glutathione sepharose beads

To generate baits for the pull-down experiment, *GST-AIP1-1* and *GST-AIP1-2* construct carried by pETGST vector (Fig. 6) were transformed into *E. coli* as described above (see 3.3.2.) and expressed using an auto-induction system. As a negative control for the pull-down experiment, pETGST vector, carrying GST alone was also transformed into *E. coli* and expressed using the auto-induction system.

The principle of the auto-induction is based on the preference of bacteria to use glucose over lactose (galactose) as a primary energy source (Studier, 2005). The medium used contains a small amount of glucose. Once the glucose is used up, lactose becomes the main energy source in the

medium, and the bacteria adapt by changing their metabolism to use lactose (Studier, 2005). The genome of bacteria like Rosetta (DE3) used in our study has been complemented with a gene consisting of the lac operator driving the expression of a gene controlled by the T7 promoter. Therefore, the switch to lactose metabolism induces the production of the target protein controlled by the T7 promoter. This is because lactose interferes with lac repressor binding to the lac operator thus promoting T7 RNA polymerase binding to T7 promoter in order to express the gene of interest (Studier, 2005).

A single colony of *E. coli* transformed with pETGST vector carrying *GST-AIP1-1*, *GST-AIP1-2* construct, or GST alone (see 3.3.2) was inoculated into 3 ml of auto-induction medium (Tab. 2) followed by incubation for 3 h at 37 °C with agitation at 210 rpm. The culture was then incubated for 16 h at 20 °C with agitation at 210 rpm.

The following steps of protein extraction and protein binding to beads were performed either on ice or at 6 °C. The cells were harvested by centrifugation for 1 min at 18.000 g and the pellet was resuspended in 300 µl PBS that helps to maintain the constant pH, supplemented with 1x protease inhibitor cocktail (Sigma) and 1mM PMSF to prevent protein degradation. The cells were lysed using a Vibra-Cell™ sonicator (Sonics) with a pulse protocol of 3x12 s with a 15 s interval and 40% amplitude until the lysate was clear. After adding Triton X-100 to a final of 1% concentration, 300 µl lysate was centrifuged 10 min at 15.000 g and the supernatant was collected for next steps.

We next coupled GST-AIP-1-1 and GST-AIP1-2 fusion protein as well as GST alone to the beads. Three hundred microliters of supernatant containing GST-AIP-1-1 and GST-AIP1-2 and 15 µl supernatant containing GST alone were incubated with 40 µl of beads prepared as indicated below (see 3.6.1), for 1 h on a rotating wheel. The beads were then collected by centrifugation for 5 min with 500 g and the supernatant was discarded. As a negative control during the pull-down assay, 40 µl beads prepared as indicated above (see 3.6.1), were also included in following steps without being subjected to any bacterial extracts. To prevent unspecific binding of protein to the bead during the pull-down, the beads were blocked for 30 min in PBS containing 1% low-fat milk powder and 1% Triton X-100. Subsequently, the beads were washed 2x5 min in PBS containing 1% Triton X-100. The beads were always washed on a rotating wheel and between each wash step the beads were centrifuged at 500 g for 5 min and the supernatant was discarded.

The beads were then blocked a second time in PBS containing 2% Bovine serum albumin (BSA) and 1% Triton X-100. Subsequently, the beads were centrifuged at 500 g for 5 min and the supernatant was discarded. The beads were then washed 1x5 min in PBS containing 1% Triton X-100, centrifuged 5 min at 500 g and the supernatant was discarded. After this step, the beads were ready for use in pull-down experiments.

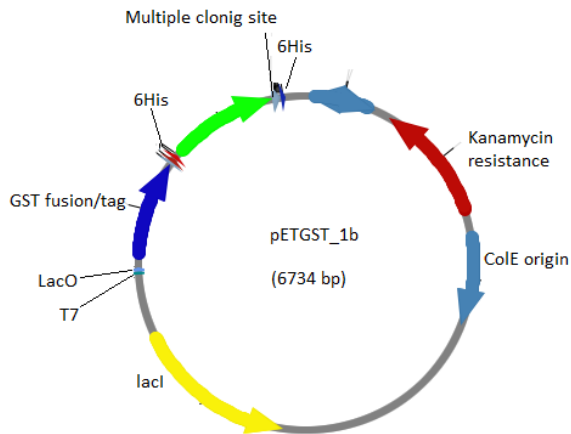


Figure 6: Vector map of pETGST_1b used to clone the cDNA encoding for AIP1-1 or AIP1-2 as an in-frame fusion to the GST tag coding sequence. Lac I encodes the lac repressor; lac operator (lacO) is located downstream of the T7 promoter (T7); 6xHistidine tag (6His); Multiple cloning site for cloning; Kanamycin resistance as a selectable marker and ColE origin for replication in *E. coli*.

3.5.2. Extraction of plant protein for the pull-down experiments

Prior to this study, a root suspension culture of *Arabidopsis thaliana* Col-0 had been generated that was made kindly available by Dr. László Bakó. To generate the plant extracts for the pull-down experiment, a suspension culture was subcultured in MSAR medium (Tab. 2) for three to four days under agitation at 120 rpm in an *in vitro* growth chamber with the growth conditions described below (see 3.7.1). After having reached the logarithmic growth phase, the suspension was filtered through a Miracloth filter using a water-jet vacuum pump, an Erlenmeyer flask with vacuum release and a Buchner funnel. The suspension was frozen in liquid nitrogen and 2 g were mixed with 6 ml ice cold bead-binding buffer (Tab. 1) containing 1x plant protease inhibitor (Sigma) cocktail and 1 mM PMSF. The following steps of protein extraction were performed

either on ice or at 4 °C. The cell suspension was sonicated 2-3x15 s with 15 s interval and 40% amplitude to disrupt cells and then mixed with 6 ml bead-binding buffer supplemented with 10% glycerol, 2% Triton X-100 and 1 mM DTT. After 10 min of centrifugation at 10.000 g, the supernatant was transferred to a new tube and centrifuged again for 10 min at 30.000 g. The supernatant was collected and used in the pull-down experiments.

3.5.3. Expression of His-ACT2 and His-ACT7 using an IPTG induction system

To obtain extracts of bacteria expressing 6xHis-ACT2 or 6xHis-ACT7 for pull-down experiments, *6xHis-ACT2* or *6xHis-ACT7* constructs carried by the pCold I vector (Fig. 7) were transformed into *E. coli* cells as described above (see 3.3.2), and expressed using the Isopropyl β -D-1-thiogalactopyranoside (IPTG) induction system. As a negative control for 6xHis-ACT2 or 6xHis-ACT7 expression, empty pCold I vector was also transformed in *E. coli* and expressed using IPTG induction system.

Briefly, IPTG induction is based on the presence of T7 RNA polymerase that binds specifically to T7 promoter to promote the expression of genes under control of the T7 promoter (Studier, 2005). The lac repressor can bind to the lac operator located downstream of the T7 promoter and in this way it inhibits T7 RNA polymerase binding to T7 promoter thus repressing the expression of the gene under control of the T7 promoter. When IPTG is present, it interferes with the binding of the lac repressor to lac operator, thus allowing binding of T7 RNA polymerase and expression of the gene under control of T7 promoter (Studier, 2005).

One colony was inoculated in 5 ml of LB and the suspension was grown under agitation at 230 rpm at 37 °C for 4 h and then cooled down at 15 °C for 30 min as a cold shock. Expression of 6xHis-ACT2 or 6xHis-ACT7 was induced by addition of 50 μ M IPTG. The cell suspension was kept at 15 °C for 20 h under agitation at 230 rpm and cells were harvested by centrifugation at 18.000 g for 1 min. The cells were frozen at -80 °C for a minimum of 2 h. After, the cells were then resuspended in buffer A (Tab. 1) and lysed using a sonication routine of 4x15 s pulses with 20 s intervals at 40% amplitude. The lysate was centrifuged at 15.000 g for 10 min at 4 °C, the supernatant was collected and used in pull-down experiments. The expression of 6xHis-ACT2 or

6xHis-ACT7 was tested by Coomassie staining and immunodetection on Western blots as described above (see 3.4.3 and 3.4.4). In Western-blot experiments, 6xHis-ACT2 or 6xHis-ACT7 expression was analyzed using anti-actin-11 antibody (Tab. 5) followed by membrane stripping and detection with anti-6xHis antibody (Tab. 5).

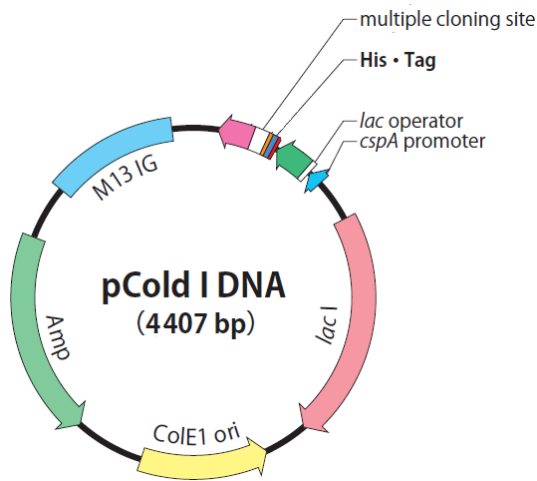


Figure 7: Vector map of pCold I used to clone *ACT2* or *ACT7* as a fusion to a 6xHis-tag. *lac I* encodes the lac repressor; the *lac* operator (*lacO*) is situated downstream of the *cold shock promoter* (*cspA*); 6xHistidine-tag (His); multiple cloning site for cloning; intergenic sequence of M13 bacteriophage (M13 IG), Ampicillin resistance (Amp) which is the selectable marker and ColE origin for replication in *E. coli*.

3.5.4. Protein extraction from plants expressing *gAIP1-2-Venus* or *gAIP1-2-mCherry*

To analyze the expression level of fluorescently tagged AIP1-2 in plants expressing *gAIP1-2-Venus* or *gAIP1-2-mCherry* under control of their endogenous genomic regulatory sequences in the Col-0 background, proteins were extracted from five-day-old seedlings. Five seedlings were placed in Eppendorf tubes and after addition of 50 μ l ice-cold extraction buffer (Tab. 1), seedlings were roughly ground using a precooled pestle. One hundred and fifty microliters of ice-cold extraction buffer was then added to the homogenized sample that was finely ground using a grinding machine (Black & Decker). The sample was centrifuged at 10.000 g for 10 min at 4 °C and the supernatant was collected. After performing the Bradford assay as described above (see 3.41.1), 25 μ g of the supernatant was mixed with the 1x SDS

loading buffer (Tab. 1), heated at 95 °C for 5 min, and cooled down prior to loading on an SDS PAGE gel as indicated above (see 3.4.2). For Western blot analysis, anti-actin-11 antibody (Tab. 5) was used to verify equal loading of proteins on SDS PAGE gel whereas anti-RFP antibody (Tab. 5) and anti-GFP antibody (Tab. 5) were used to analyze expression of gAIP1-2-mCherry and gAIP1-2-Venus respectively.

3.6. GST pull-down experiments

GST pull-down experiments are a valuable *in vitro* method that is commonly used to analyze interaction between two or more proteins (Einarson *et al.*, 2007). To determine interaction in the pull-down experiment, one of the proteins of interest, often referred to as the “bait”, is immobilized to a solid phase support (Einarson *et al.*, 2007). In our study, the bait immobilization is possible because the bait protein (AIP1-1 or AIP1-2) is fused to Glutathione-S-transferase (GST), whereas the solid phase support, the bead, contains glutathione, a substrate of GST (Fig. 8). After washing to remove unbound protein, the immobilized bait is incubated with prey protein containing solution. The unbound proteins are removed by washing and the bait-prey complex is eluted from the solid-phase support (Einarson *et al.*, 2007). The results are examined using SDS-PAGE followed by Coomassie stain and by Western blotting using an antibody that is specific to the prey protein (Fig. 8) (Einarson *et al.*, 2007).

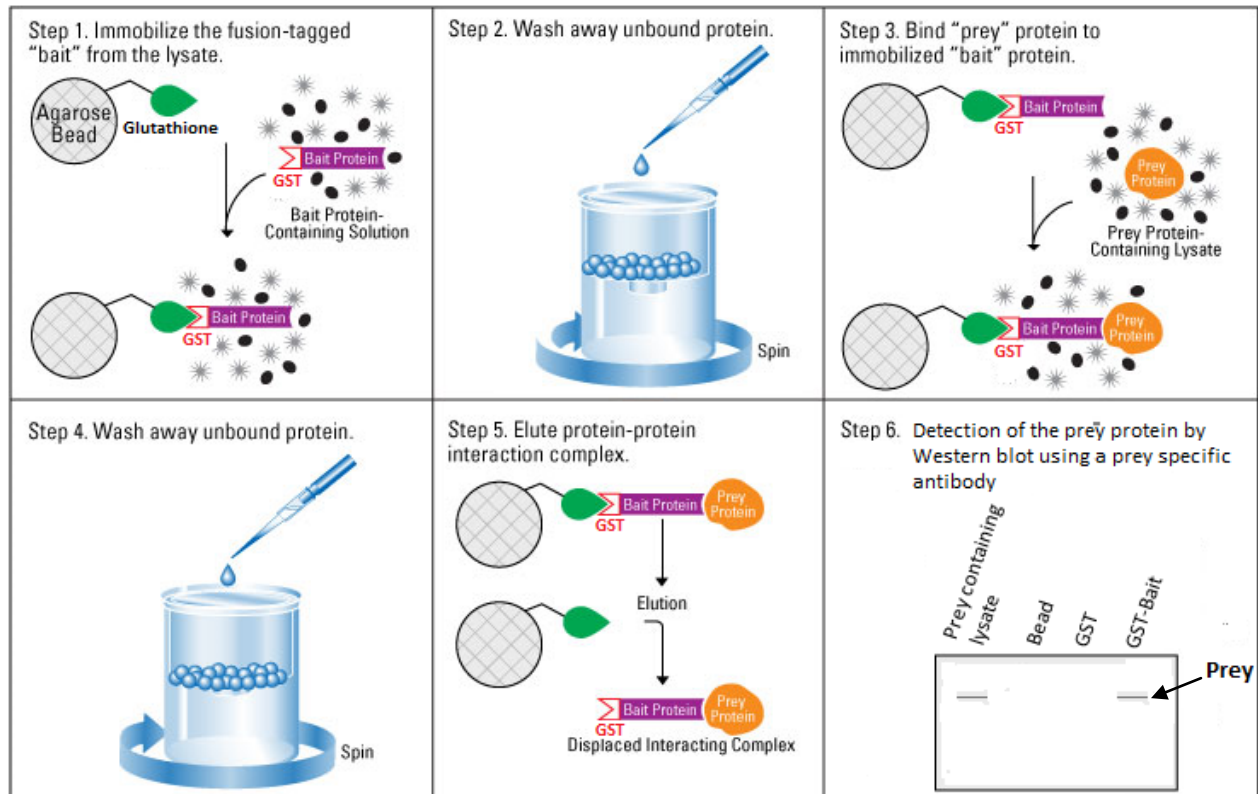


Figure 8: A GST pull-down experiment using bead-coupled bait protein to precipitate the prey protein (adapted from Einarson *et al.*, 2007).

3.6.1. Preparation of glutathione sepharose beads

Prior to the coupling of GST-AIP1-1, GST-AIP-2 or GST alone to Glutathione Sepharose beads (GE Healthcare) as described above (see 3.5.1.), glutathione sepharose beads were prepared as follows. Forty microliters of the beads were transferred into Eppendorf tubes. To wash the beads, 400 μ l PBS were added to the tubes and the suspensions mixed by inversion. The tubes were then centrifuged at 500 g for 5 min and the supernatant was discarded. The wash and centrifugation steps were repeated once and the supernatant was discarded. The beads were ready to be linked to GST-AIP1-1, GST-AIP1-2 or GST alone.

3.6.2. *In vitro* binding assay

We performed an *in vitro* binding assay using GST-AIP1-1 or GST-AIP1-2 as the bait, and plant or bacteria extracts containing the appropriate prey. Three hundred microliters plant or bacteria protein extracts was added to the beads coated with GST-AIP1-1 or GST-AIP1-2 and the mixture was incubated for 2 h rotating at 6 °C. The beads coated with GST alone and the beads alone were used as negative controls and were subjected to the same conditions and treatments as the beads coated with GST-AIP1-1 or GST-AIP1-2. After incubation with plant protein extracts, the beads were washed 3x 10 min in bead binding buffer containing 1% triton X-100 and 5% glycerol rotating at 6 °C. Each step of washing was followed by centrifugation with 500 g for 5 min at 4 °C and the supernatant was discarded. After the last removal of supernatant, 40 µl of 5x SDS sample buffer was added to the beads and the mixture was heated at 95 °C for 5 min. The mixture was then centrifuged with 15.000 g for 1 min and the supernatant collected for analysis using SDS-PAGE followed by Coomassie and Western blot as described above (see 3.4.2, 3.4.3 and 3.4.4). In Western-blot experiments, to analyze pulled down actin, anti-actin-11 antibody (Tab. 5) was employed, followed by membrane stripping and detection with anti-GST antibody (Tab. 5) to determine GST fusion proteins.

3.7. Plants growth and materials

3.7.1. Plant growth conditions

The plant used in our study was *Arabidopsis thaliana*. Seeds were dried one week at 37 °C to facilitate germination and sterilized before plating. For sterilization seeds were placed in Eppendorf tubes and 650 µl sterilization solution (Tab. 1) was added and removed after 1-3 min. 850 µl 1x Bayrochlor solution (Tab. 1) was added for 12-15 min and the tube was inverted occasionally. The Bayrochlor solution was then removed and seeds were washed twice with 1 ml sterile H₂O. Ultimately, 500 µl H₂O were added and seeds were kept at 4 °C for three to five days in the dark for stratification. Seeds were then plated on MS agar (Tab. 2), plates positioned vertically and transferred to an *in vitro* culture room under 16 h light (around 150 µmol/m²s) and

8 h of darkness under 60% of humidity at around 22 °C. To have a control, transgenic lines were grown on the same plates with the wild type. After five days, seedlings were ready for analysis.

Five-day-old seedlings for use of *Agrobacterium* transformation, for crossing as well as for BASTA selection were initially grown on MS agar and were then transferred to a general-purpose compost (P-jord)-Vermiculite (4:1) mixture. To avoid the growth of syrphid fly larvae, this soil mixture was sprayed with nematode (*Steinernema feltiae*) egg solution (NEMAbloom). Growth conditions of plants in growth chambers were similar to those of *in vitro* chamber grown plants with 70% humidity. The trays containing seedlings were covered with a top cover that was removed after four days of acclimatization and trays were watered every three to four days.

3.7.2. BASTA selection of plants after *Agrobacterium* transformation

After transformation of a plasmid vector carrying a construct encoding for ER-resident mCherry under control of the native *AIP1-2* genomic region into *Arabidopsis*, transformed plants were selected using BASTA (0.25 g/l). Three weeks after transformation, seeds were harvested and cultured on the soil surface of the tray that was then covered and kept at 4 °C for 2-3 days. Subsequently, the plants were moved to a growth room with long-day growth conditions as mentioned above (see 3.7.1.). Once the cotyledons had clearly developed, BASTA was applied the first time by spraying and the treatment was repeated twice within seven-day intervals. Resistant plants were transferred to pots and were grown in long-day conditions until seeds were produced after approximately three weeks.

3.7.3. Crossing T2 plants expressing *gAIP1-2-Venus* and *gAIP1-2-mCherry*

In this study, we started off with T2 plants each containing four copies of *AIP1-2* that are two copies of the endogenous, native gene and two copies of a transgene expressing *AIP1-2* fused to a fluorescent protein from genomic *AIP1-2* (*gAIP1-2*) coding sequences. To generate plants containing six copies of *AIP1-2*, we crossed plants expressing *gAIP1-2-Venus* and

gAIP1-2-mCherry in Col-0 background. After epifluorescence microscope analysis as described below (see 3.8.1.1.), strongly fluorescing plants were selected for crosses. To this end, we used flowers of the female parent before anthers started to release pollen to stigma and the open flowers of the male parent with anthers releasing pollen. The flower of the mother plant was emasculated by removing sepals, petals and anthers with fine forceps and only leaving the carpel. Pollens from the male partners were transferred by squeezing the flower using forceps, and anthers were brushed over the stigma of the female parent flower. After crossing, plants were grown under long-day conditions as mentioned above (see 3.7.1) until seeds could be harvested after approximately three weeks.

3.8. Microscope

3.8.1. Fluorescence microscopy

Fluorescence microscopy relies on that fluorescence molecules can absorb light of certain wavelength and emit light at longer wavelength and of different color that can be detected as fluorescence (Fine, 2007). When fluorescent molecules are present in a specimen or are artificially introduced, the specimen can be visualized by fluorescence microscopy (Fine, 2007).

3.8.1.1. Epifluorescence microscopy

To detect images by epifluorescence microscopy, the light from mercury-vapor lamp, a commonly used light source, is filtered by an excitation filter to select the wavelength required to excite the specimen, and then reflected by dichroic mirror towards the specimen through the objective (Fine, 2007). Fluorescence of excited molecules in the specimen is then collected by the objective, passed through the dichroic mirror to select emitted fluorescence light, and through an emission filter to allow a certain wavelength light to pass before reaching the microscopy eyepieces or the camera for detection. To change excitation wavelength quickly, excitation filter can be replaced by an external filter wheel containing different filters (Fine, 2007).

The epifluorescence stereomicroscopy employed in this study was a Leica MZ FLIII. In order to analyze the segregation ratio of T2 plants expressing *gAIP1-2-Venus* or *gAIP1-2-mCherry* in the Col-0 background, a GFP filter or an RFP filter was employed and plants with strong fluorescence were selected and grown for crosses. After crossing as described above (7.3.), we selected plants with strong fluorescence for both Venus and mCherry to be used in root hair positioning analysis. Each plant was examined first with the GFP filter and secondly with the RFP filter.

3.8.1.2. Confocal microscopy

Confocal laser scanning microscopy (CLSM) is a type of fluorescent microscopy that increases the resolution of the specimen by illuminating one point of the specimen and uses the pinholes to eliminate light from above or below the focal plane (Fine, 2007). Using this approach of one point illumination, images from different position in Z position allow to build a 3 dimensional image of the specimen (Fine, 2007). To detect images by CSLM, excitation light is provided by the laser of specific wavelength, and reflected by the dichroic mirror, encounters the pinhole and reaches the specimen via mirrors. Fluorescence of excited molecules in the specimen passes through the dichroic mirror, encounters the pinhole and finally reaches the detector which is commonly a photomultiplier tube. When a specimen contains two different fluorescence molecules, two lasers of different wavelength can be used together and generate a multicolor image (Fine, 2007).

We used a Zeiss LSM780 confocal microscope employing Zeiss ZEN2010 software. All seedlings were analyzed using a 40x water immersion objective. To prepare samples, five-day-old seedlings were placed on a microscope slide containing a drop of MS medium, flanked by two strips of double-sided adhesive tape and were covered by a long cover slip that was gently pressed on the adhesive tape. To keep the seedlings under moist conditions during analysis, MS medium was continuously added at the ends of the coverslips.

Strongly fluorescing T2 plants expressing *gAIP1-2-Venus* and *gAIP1-2-mCherry* used for crossing as described above (see 3.7.3) were also analyzed using CLSM. An excitation

wavelength of 514 nm was employed for plants expressing *gAIP1-2-Venus* whereas 561 nm was used for plant expressing *gAIP1-2-mCherry*. To eliminate any detection of mCherry in the Venus emission spectrum and vice versa, we performed a lambda scan of the mCherry line using the laser settings used for Venus detection and vice versa. The spectral region of the lambda scan was 446-608 nm with 8 nm intervals. After crossing, plants that showed strong fluorescence using epifluorescence microscopy were also examined by CLSM prior to analysis of root hair positioning.

To analyze the expression pattern of an ER-resident mCherry construct under control of the native *AIP1-2* genomic region using CLSM excitation at 561 nm was employed. To determine the appropriate emission spectrum and eliminate unspecific signal, a lambda scan of the wild type using the laser settings employed for the transgenic plant was performed. The spectral region of lambda scan was 446-608 nm with 8 nm intervals.

3.8.2. Light microscopy analysis of root hair positioning

We examined root hair positioning of plants that showed strong fluorescence that were obtained from crosses between plants expressing *gAIP1-2-Venus* and *gAIP1-2-mCherry* as described above (see 3.7.3). An Axioplan 2 microscope (Zeiss) was used for these analyses. Roots were observed using the 40x lens and pictures were acquired using AxioCam digital camera and Axiovision 3.1 software. For these experiments, seeds were sterilized and plated as described above (see 3.7.1). Seedlings were then put in 12-well culture plates containing 1 ml of Ethanol: clearing solution (7: 3 ratio) (Tab. 1) and were incubated for 30 min. The Ethanol: clearing solution was removed and 1 ml clearing solution (Tab. 1) was added, left and removed after 30 min of incubation. Seedlings to be analyzed were placed on microscope slides covered with clearing solution and the cover slide was added on the top. The first ten cells closest to the root tip and the 10 cells closest to the hypocotyl-root junction were excluded from these analyses.

4. Results

4.1. Analysis of interaction between AIP1-1 or AIP1-2 and actins

4.1.1. GST-AIP1-1 and GST-AIP1-2 precipitate actins from plant extracts

To address whether AIP1-1 or AIP1-2 can interact with actins at the protein level, pull-down experiments were conducted by incubating plant protein extracts with the beads carrying GST-AIP1-1, GST-AIP1-2, GST alone or pure beads. GST-AIP1-1, GST-AIP1-2 and GST were expressed in bacteria, loaded to the bead and subjected to *Arabidopsis* protein extracts obtained from a root cell suspension culture. After the pull-down step, the beads covered with proteins from the precipitation, were washed and then boiled in the presence of SDS buffer. Aliquots of the obtained solution were separated by SDS-PAGE for subsequent analysis by Coomassie staining and immunoblotting. Analysis of the Coomassie stained gel revealed that bacteria expressing GST-AIP1-1 or GST-AIP1-2 displayed a band of approximately 93 kDa corresponding to the size of the GST-AIP1-1 or the GST-AIP1-2 fusion proteins, whereas bacteria expressing GST displayed a band of about 26 kDa corresponding to the size of GST protein (Fig. 9C). This indicated that GST-AIP1-1 or GST-AIP1-2, and GST were expressed in *E. coli* cells and that the proteins were successfully coupled to the beads. Western blot analysis of cell suspension protein extracts with an anti-actin-11 antibody, revealed a band of approximately 42 kDa which is equivalent to the size of monomeric actin confirming recognition of actin in plant protein extracts used in this experiment (Fig. 9A). Whereas protein extracts recovered after incubation with pure beads or beads with GST adsorbed did not show a band of the size of actin when probed with an anti-actin-11 antibody, extracts recovered after incubation with GST-AIP1-1 or GST-AIP1-2 loaded beads, showed a band corresponding to the size of actin (Fig. 9A). To examine the identity of additional cross-reacting bands observed on anti-actin-11 blot, the blot was additionally probed with an anti-GST antibody. The observed GST, GST-AIP1-1 and GST-AIP1-2 bands indicated that the cross-reacting bands apparent on the anti-actin-11 Western blot are due to the high amount of GST (-fusion) proteins that unspecifically bound the antibody in addition to the specific recognition of actin (Fig. 9B, 9C). In summary,

these results revealed that GST-AIP1-1 or GST-AIP1-2 can specifically pull down actins from plant extracts.

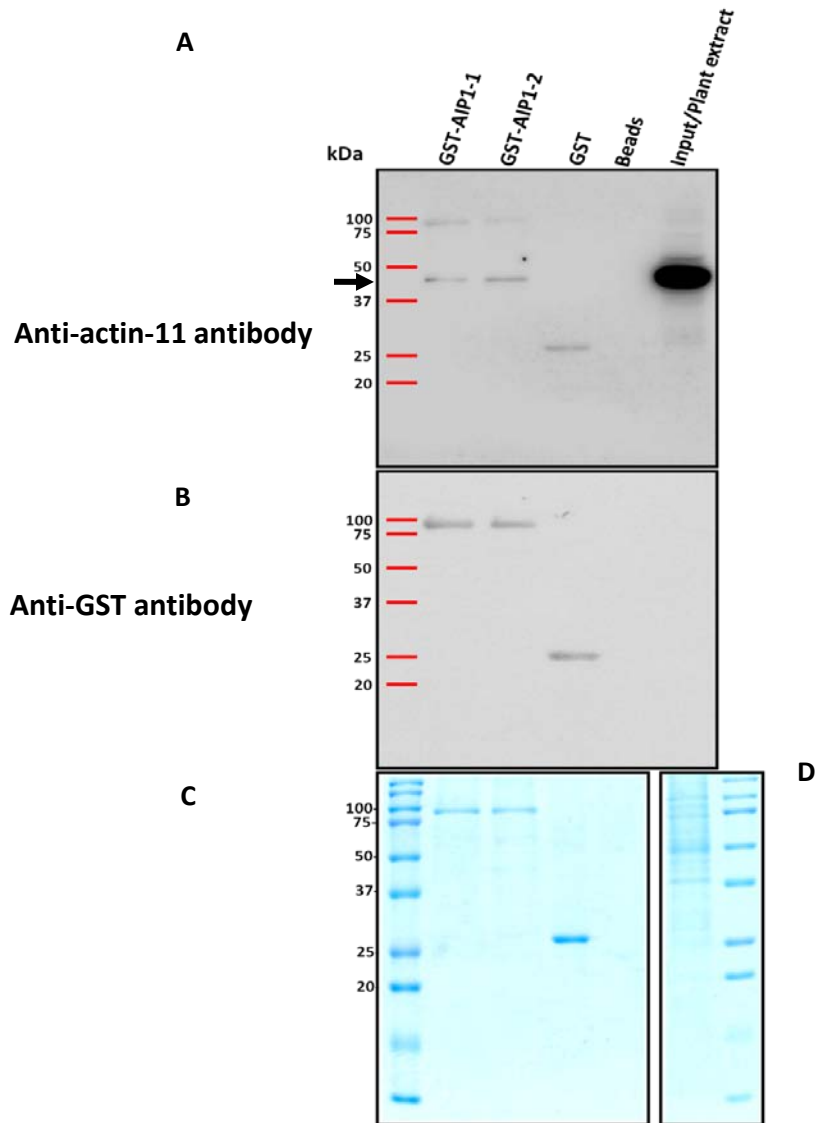


Figure 9. GST-AIP1-1 and GST-AIP1-2 pulled down actin from *Arabidopsis* root cell suspension protein extracts. **(A)** Blot after pull-down experiment probed with anti-actin-11 antibody. Lane 1 (from the left) shows the molecular weight markers. Bait proteins adsorbed to the beads and the beads alone are indicated on the top in lane 2 to 4. Lane 5 shows 1/50 of plant extracts used in the pull-down experiment. **(B)** Blot after pull-down experiment probed with anti-GST antibody. Black arrow shows actin bands **(C)** Coomassie brilliant blue-stained gel revealing the presence and amount of bacterially expressed proteins retained on glutathione sepharose beads. **(D)** Coomassie brilliant blue stained gel showing *Arabidopsis* root cell suspension protein extracts. Similar results were obtained from four independent pull-down experiments.

4.1.2. His-ACT2 and His-ACT7 expression in Rosetta (DE3) cells.

To test whether AIP1-2 can interact specifically with ACT2 or ACT7, we first aimed to express 6xHistidine (His)-tagged ACT2 (His-ACT2) or His-ACT7 in *E. coli*. This could provide extracts containing His-ACT2 or His-ACT7 as the sole actins for the pull-down experiment. Expression of actin in *E. coli* encounters different obstacles such as the ability of actin to polymerize as well as potential incomplete folding of the protein. The pCold I vector has previously been used to express non-plant actin and was therefore employed in this study to attempt to express His-ACT2 or His-ACT7 using the IPTG induction system (Tamura, *et al.*, 2011). Bacterial extracts obtained from cultures grown as described in 3.5.3 were subjected to SDS-PAGE and separated for analysis by Coomassie staining and immunoblotting. Analysis of Coomassie stained gels revealed weak bands of about 43 kDa corresponding to the size of His-actin in bacterial extracts of lines containing the *His-ACT2* or *His-ACT7*-coding vector, but not in lines containing the empty vector used as a negative control (Fig. 10C). To further investigate the expression of His-ACT2 or His-ACT7, Western-blot analysis was performed. When probing the blot with the anti-actin-11 antibody, a band of His-ACT2/7 size was observed in bacterial extracts containing His-ACT2 or His-ACT7 similar to the result observed for the plant extracts but in clear contrast to extracts from bacteria carrying only the empty pCold I vector (Fig. 10A). After stripping, the membrane was reprobed with anti-His antibody, revealing a protein band of His-actin size in the extracts of bacteria expressing His-ACT2 or His-ACT7 but not in plant extracts or in extracts from *E. coli* transformed with the empty pCold I vector (Fig. 10B). Taken together, these results showed that recombinant His-ACT2 and His-ACT7 could be successfully expressed in *E. coli*, providing bacterial protein extracts containing His-ACT2 or His-ACT7 as the sole actin to be used for pull-down experiments.

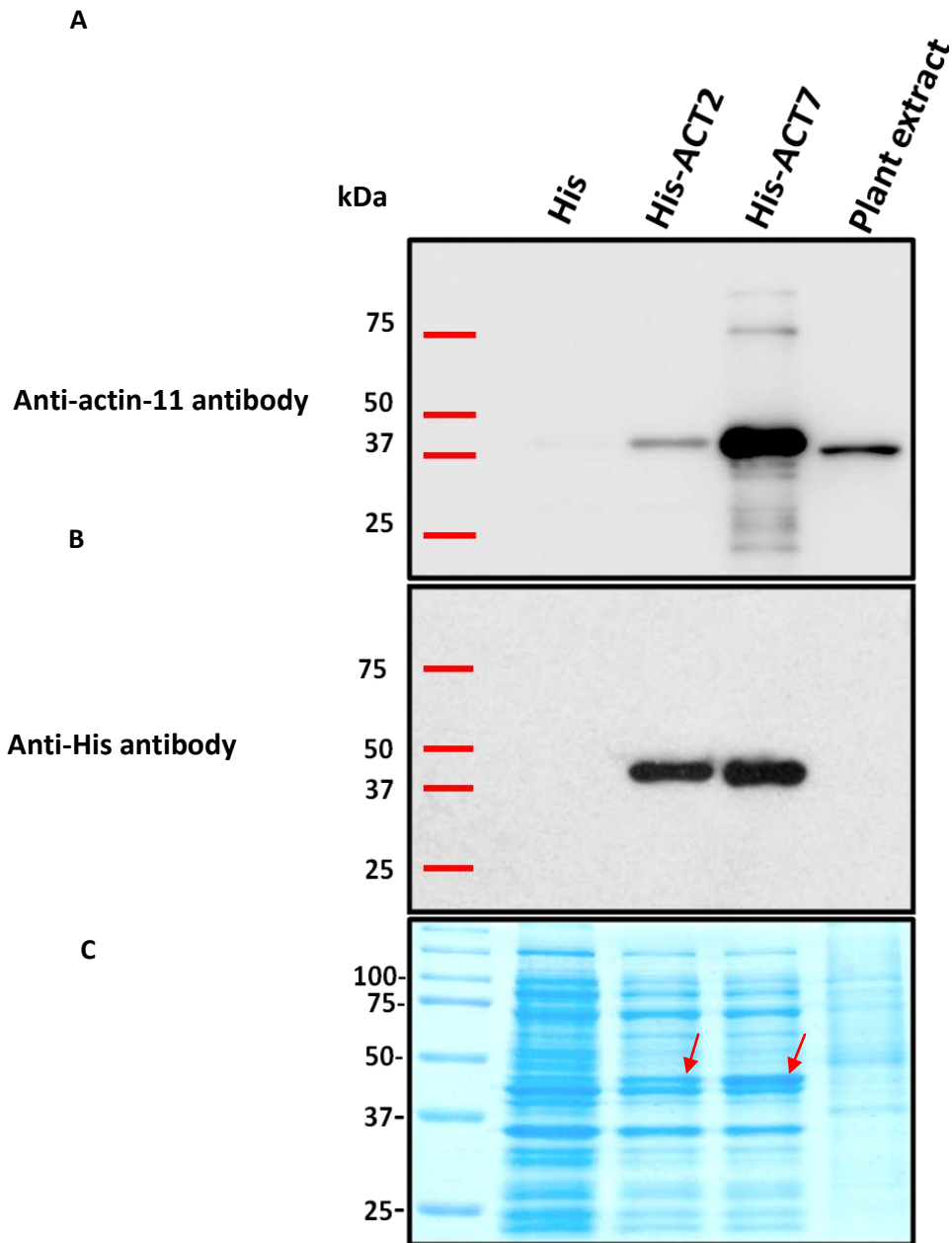


Figure 10. Expression of His-ACT2 or His-ACT7 in *E. coli*. **(A)** Blot probed with anti-actin-11 antibody. Lane 1 (from the left) shows the molecular weight markers. Top label indicates the His-fusion proteins contained in the bacterial extracts (Lane 2 to 4). Lane 5 shows plant extracts as a positive control for the presence of actin. **(B)** Blot probed with anti-His antibody. **(C)** Coomassie brilliant blue-stained gel containing bacterial or plant protein extracts. Red arrows show the bands of the actin size.

4.1.3. GST-AIP1-2 precipitates His-ACT7 from bacterial protein extracts

Initially, AIP1-2 was tested for interaction with ACT7 in the *in vitro* pull-down assay. GST-AIP1-2 and GST alone expressed in *E. coli*, were coupled to beads and incubated with bacterial extracts containing His-ACT7. After incubation, the absorbed proteins were eluted by boiling with SDS, separated via SDS-PAGE and analyzed by Coomassie staining and immunoblotting. As negative controls, extracts from bacteria containing empty pCold I vector were incubated with the same beads. Analysis of the Coomassie Brilliant Blue-stained gel revealed that GST-AIP1-2 and GST alone were expressed and attached efficiently to the beads and both showed the same amount of protein (Fig. 11C). Probing the corresponding Western blot with anti-actin-11 antibody revealed the band of expected actin size in bacterial extracts expressing His-ACT7 but not in extracts of bacteria containing empty pCold I vector showing that His-ACT7 was successfully expressed (Fig. 11A). Western blot analysis using anti-actin-11 antibody showed that only GST-AIP1-2 was able to specifically pull down His-ACT7 from the bacterial extract, as observed by the presence of the band of actin size and the absence of the corresponding band in the GST-coupled bead and empty bead control reactions (Fig. 11A). Analysis of Western blots using anti-GST antibody revealed loading of an equal amount of GST and GST-AIP1-2 (Fig. 11B). Together, these findings indicated that GST-AIP1-2 specifically bound to His-ACT7 from *E. coli* extracts.

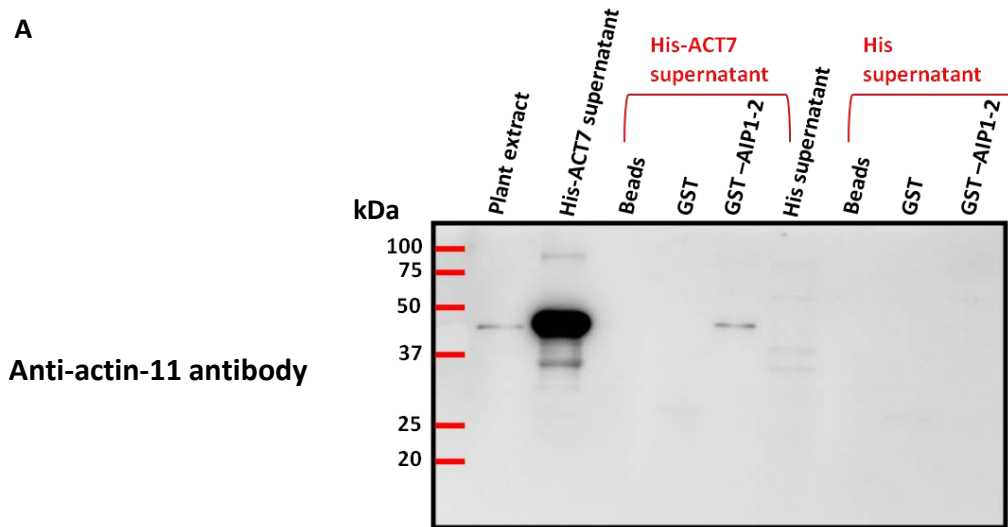
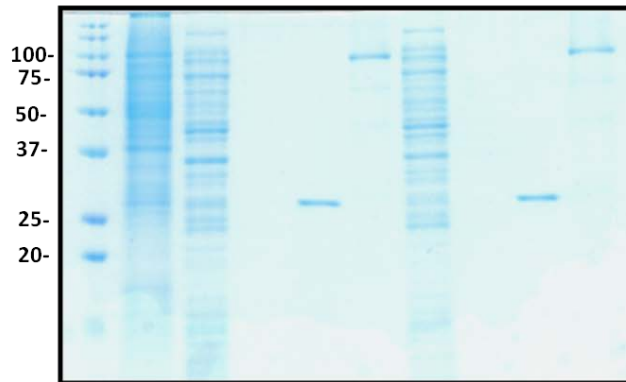
A**B****Anti-GST antibody****C**

Figure 11. GST-AIP1-2 pulled down His-ACT7 from *E. coli* extracts. **(A)** Blot after pull-down experiment probed with anti-actin-11 antibody. Lane 1 (from the left) shows the molecular weight markers. Bait proteins adsorbed to the beads and the beads alone are indicated on the top. Supernatant which is the total soluble protein fraction of *E. coli* applied to the baits coupled to the beads is shown in red color and 1/50 of supernatant used in the pull-down experiment was loaded in lane 3 and 7. Plant extracts were loaded in lane 2 as a positive control of the presence of actin. **(B)** Blot after pull-down experiment probed with anti-GST antibody. **(C)** Coomassie brilliant blue-stained gel revealing the presence and amount of bacterially expressed proteins retained on glutathione sepharose beads. Similar results were obtained in two independent pull-down experiments.

4.1.4. GST-AIP1-2 precipitates His-ACT2 from bacterial protein extracts

To address whether AIP1-2 can interact with ACT2, we used the same approach as described above (see 4.1.3), using extract from *E. coli* expressing His-ACT2. Coomassie stained gels containing precipitates after protein pull-down, showed that the amount of GST adsorbed to the beads was much higher than that of GST-AIP1-2 (Fig. 12C). However, the low amount of GST-AIP1-2 adsorbed to the bead precipitated His-ACT2 more efficiently than the GST-coupled beads and the empty beads controls as determined by Western blot analysis using anti-actin-11 antibody (Fig. 12A). This revealed the specific interaction between GST-AIP1-2 and His-ACT2. The smaller amount of His-ACT2 that bound to GST alone is most likely due to the high amount of GST in this experiment (Fig. 12B, 12C). When employing Western blot analysis using the anti-actin-11 antibody, no band was detected for all samples incubated with extracts of bacteria containing empty pCold I vector (Fig. 12A). After stripping the membrane used for anti-actin-11, reprobing with anti-GST antibody confirmed that the amount of GST alone was much higher than that of GST-AIP1-2 (Fig. 12C). In summary, the results described here showed that GST-AIP1-2 can specifically precipitate His-ACT2 from *E. coli* extracts.

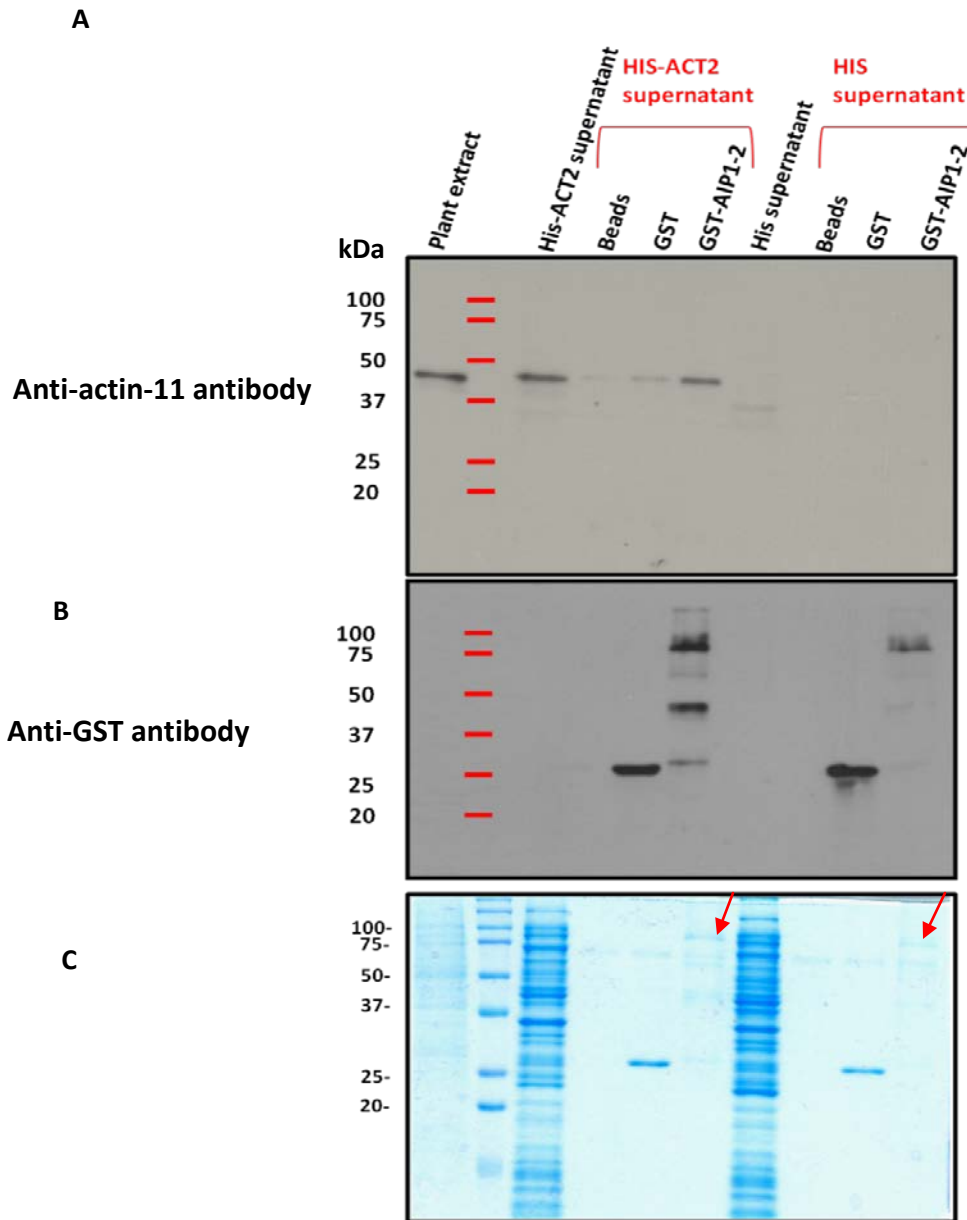


Figure 12. GST-AIP1-2 pulled down His-ACT2 actin from *E. coli* extracts. (A) Blot after pull-down experiment probed with anti-actin-11 antibody. *Arabidopsis* root cell suspension protein extract was loaded in lane 1 (from the left) as a positive control for the presence of actin. Lane 2 shows the molecular weight markers. Bait proteins adsorbed to the beads and the beads alone are indicated on the top. Supernatant which is the total soluble protein fraction of *E. coli* applied to the baits coupled to the beads is shown in red color, and 1/50 of supernatant used in the pull-down experiment was loaded in lane 3 and 7. (B) Blot after pull-down experiment probed with anti-GST antibody. (C) Coomassie brilliant blue-stained gel revealing the presence and amount of bacterially expressed proteins retained on glutathione sepharose beads. Red arrows show bands of the size of GST-AIP1-2. Similar results were obtained in two independent pull-down experiments.

4.2. Characterization of *AIP1-2* overexpressing lines

In this study, to characterize the root hair positioning phenotype of *AIP1-2* overexpression, Col-0 plants that had been transformed with *gAIP1-2-Venus* or *gAIP1-2-mCherry* and brought into the T2 generation by Christian Kiefer were subjected to further analysis.

4.2.1. Segregation analysis of fluorescent *AIP1-2* transgenes

Using an epifluorescence microscope, the segregation ratio of T2 seedlings of Col-0 background expressing *gAIP1-2-Venus* or *gAIP1-2-mCherry* was determined. Fluorescence analysis showed a ratio of about 1:2:1 (strong fluorescence: weak fluorescence: no fluorescence) for plants expressing *gAIP1-2-Venus* or *gAIP1-2-mCherry*. According to the Chi square test, this ratio did not significantly differ from the expected results of plants when each parent is heterozygous for *gAIP1-2-Venus* or *gAIP1-2-mCherry* (Fig. 13). These results indicated that transformation had led to one insertion of *gAIP1-2-Venus* or *gAIP1-2-mCherry* into the genome and that the T1 plants were heterozygous for *gAIP1-2-Venus* or *gAIP1-2-mCherry*.

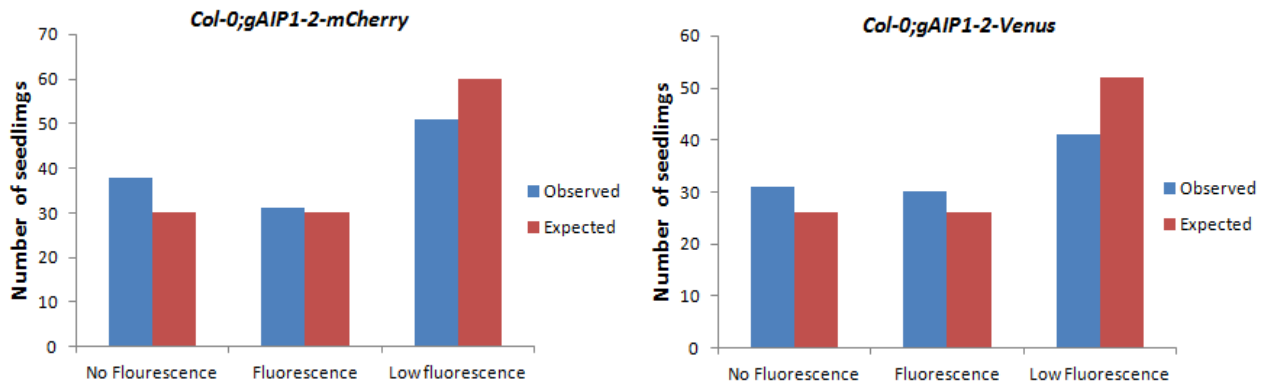


Figure 13. Segregation analysis of fluorescent protein expression in T2 generation of *gAIP1-2-mCherry* or *gAIP1-2-Venus* transformed *Arabidopsis* plants. (A) Plants expressing *gAIP1-2-Venus* in the Col-0 background. (B) Plants expressing *gAIP1-2-mCherry* in the Col-0 background. The expected ratio for heterozygous parents and observed ratio do not differ using Chi square test (*gAIP1-2-mCherry*: χ^2 (3.87) > χ^2 critical (5.9); *gAIP1-2-Venus*: χ^2 (3.51) > χ^2 critical (5.9))

4.2.2. Expression analysis of fluorescent transgenes using Western blot detection

To analyze the protein expression of T2 lines, protein extracts from five-day-old seedlings grown on MS medium were prepared, separated by SDS page and subjected to immunoblotting. Western blot analysis using anti-actin-11 antibody showed a band of actin size in the wild type, seedlings expressing gAIP1-2-Venus and gAIP1-2-mCherry (Fig. 14A). Probing the corresponding Western blot using an anti-RFP antibody showed a band corresponding to the size of gAIP1-2-mCherry at 96 kDa. This band was absent in the wild type and in seedlings expressing gAIP1-2-Venus showing the specificity of the band for gAIP1-2-mCherry expressing lines (Fig. 14B). After stripping and reprobing of the blot with anti-GFP, the antibody revealed a band with the size of gAIP1-2-Venus, 94 kDa, in extract of plants expressing gAIP1-2-Venus but not in extract from the wild type or from the plants expressing gAIP1-2-mCherry (Fig. 14C). These results confirmed the expression of gAIP1-2-Venus or gAIP1-2-mCherry and the stability of the fluorescent fusions in the analyzed lines.

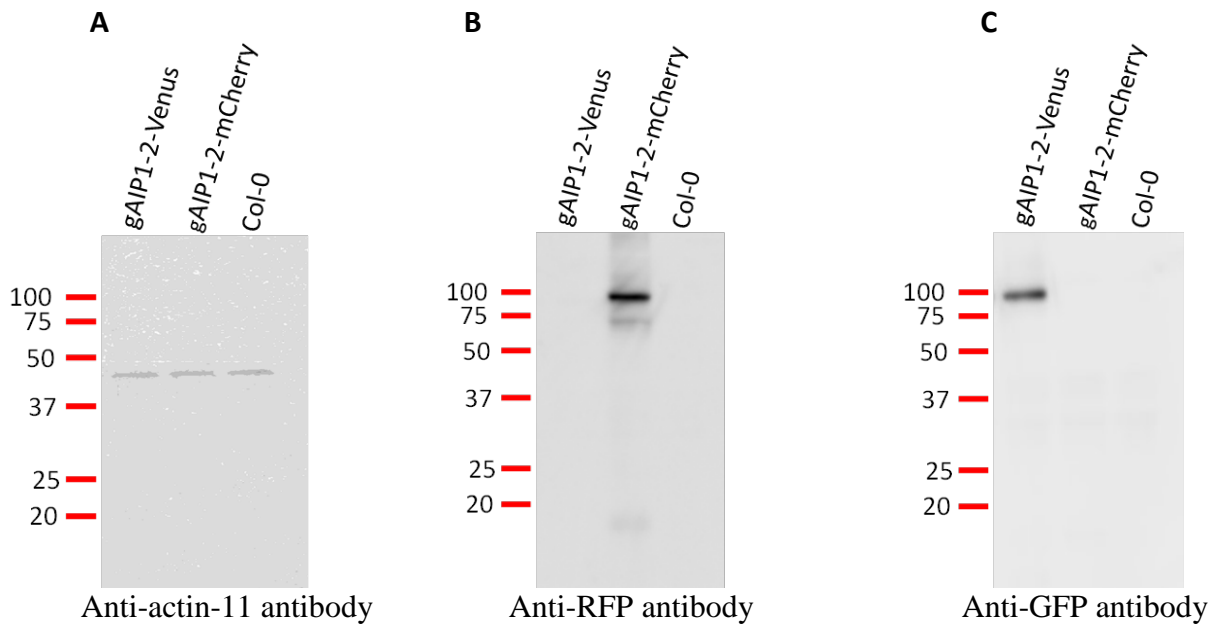


Figure 14. Western blot analysis of fluorescent protein expression in *Arabidopsis thaliana* Col-0 plants transformed with gAIP1-2-mCherry or gAIP1-2-Venus. (A) Blot probed with anti-actin-11 antibody (B) Blot probed with anti-RFP antibody. (C) Blot probed with anti-GFP antibody.

4.2.3. Generation of double transgenic lines.

To analyze the effects of *AIP1-2* overexpression, plants were generated that would carry up to six functional copies of *AIP1-2*. After prescreening for strong fluorescence, the transgenic T2 lines characterized and described above (see 4.2.1 and 4.2.2) and expressing *gAIP1-2-Venus* or *gAIP1-2-mCherry* were crossed with each other. Subsequently, F2 plants were prescreened for strong fluorescence and were used to analyze the effects of *AIP1-2* overexpression. Segregation analysis of F2 plants showed 25% of plants with strong mCherry fluorescence and 25% of plants with strong Venus fluorescence meaning that the two transgenes were not linked. In order to optimize the settings used for acquisition of the Venus spectrum, we utilized the parental plants expressing *gAIP1-2-Venus*. Lambda scan using the 514 laser (Supplementary Fig. 8.3) was performed to distinguish the spectral properties of Venus. To exclude unspecific signal, we narrowed down the detection wavelength window and collected the light in the spectral region between 516 and 551 nm, thus excluding emission of mCherry at 560 nm (Supplementary Fig. 8.2). Plants expressing *gAIP1-2-Venus* showed a strong fluorescence signal absent in the wild type, demonstrating that this signal is specific for Venus (Fig. 15A). This fluorescence was specific for hair cell files in the Col-0 background as observed in the complemented *aip1.2-1* mutant lines, indicating that *gAIP1-2-Venus* fusions behaved like in the complemented mutants and could be functional (Fig. 15A).

We optimized the settings used for acquisition of the mCherry spectrum by employing the parental *gAIP1-2-Venus* line. Lambda scan using the 561 nm laser (Supplementary Fig. 8.4) was performed to specify the spectral properties of mCherry. In order to eliminate unspecific signal, we narrowed down the detection window collecting light in the narrow spectral region between 603-630 nm and thus eliminating detection of Venus emission present at 600 nm (Supplementary Fig. 8.2). Excitation with the 561 nm laser and collection of light in the spectral region between 603-630 nm, revealed a strongly fluorescent signal in plants expressing *AIP1-2-mCherry* but not in the wild type indicating specific detection of mCherry fluorescence (Fig. 15B). Similar to the line expressing *gAIP1-2-Venus*, the fluorescence was specific to hair cell files (Fig. 15B).

Subsequently, plant expressing both *gAIP1-2-Venus* and *gAIP1-2-mCherry* were examined. In order to exclude any bleed-through of mCherry fluorescence into the Venus emission spectrum

and vice versa (Supplementary Fig. 8.5, 8.6), lambda scans of the *gAIP1-2-mCherry* expressing line using the laser settings used for Venus detection and vice versa were performed. Using both 514 nm and 561 nm laser excitation, collection of light in the spectral region between 516-551 nm, specific to Venus fluorescence revealed a strong fluorescence in double transgenic lines but not in the wild type (Fig. 15C). Collection of light using 603-630 nm, specific to mCherry showed a strong fluorescence in double transgenic lines in contrast to the wild type (Fig. 15C). These results showed that double transgenic lines were expressing *gAIP1-2-Venus* and *gAIP1-2-mCherry* and, therefore, can likely be used to analyze the planar polarity of root hair when *AIP1-2* is overexpressed.

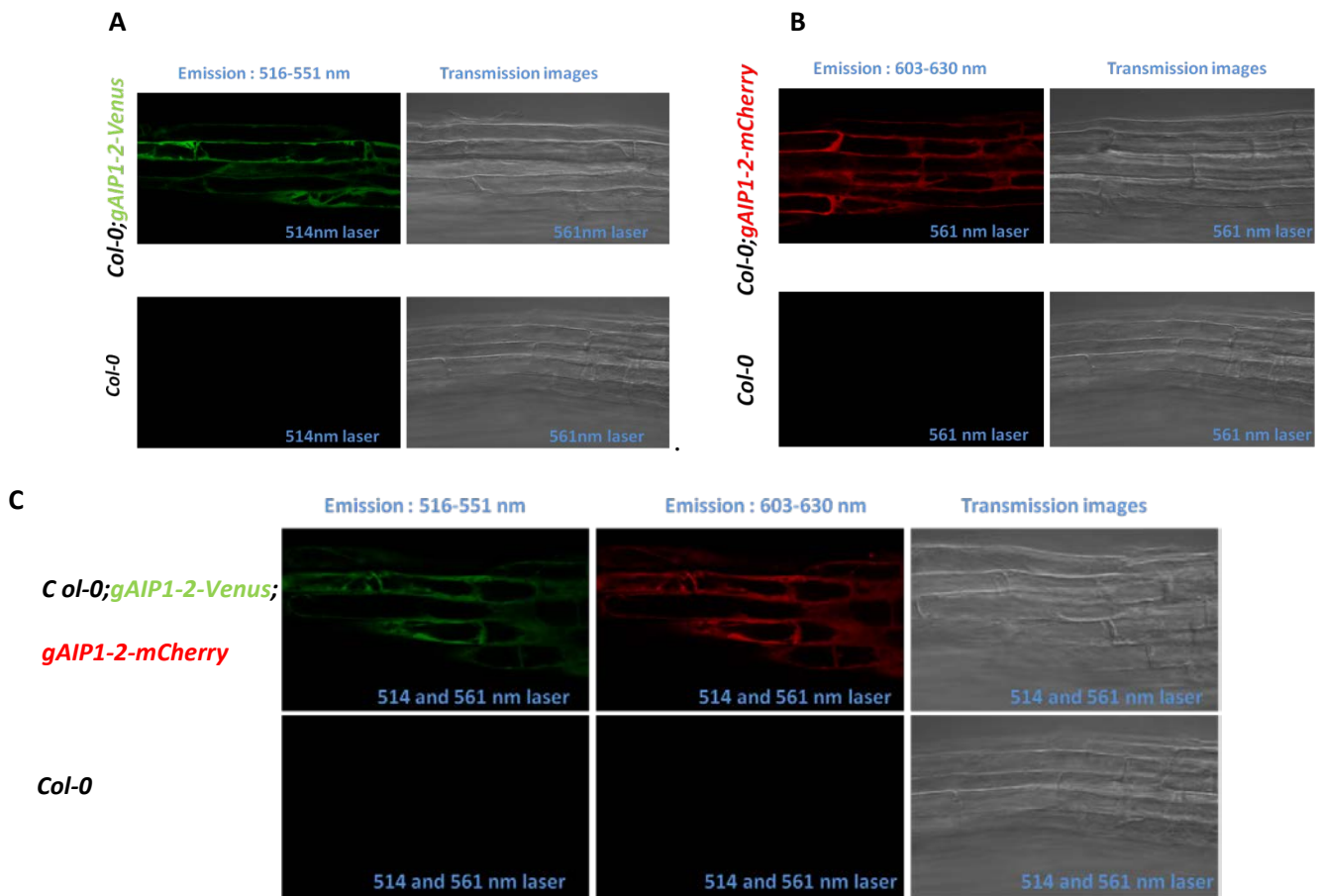


Figure 15. CLSM analysis of fluorescent *AIP1-2*-fusion expression in roots of five-day-old seedlings. **(A)** Plant expressing *gAIP1-2-Venus*. **(B)** Plant expressing *gAIP1-2-mCherry*. **(C)** Plant expressing *gAIP1-2-Venus* and *gAIP1-2-mCherry* in *Col-0* background. The laser and emission wavelengths used for CLSM analysis are displayed inside and on the top of the pictures, respectively.

4.2.4. Preliminary analysis of root hair-positioning phenotypes of AIP1-2-Venus and AIP1-2-mCherry expressing lines.

Subsequently, root hair positioning of AIP1-2-mCherry and AIP1-2-Venus expressing seedlings was analyzed by microscopy. In a few seedlings examined, root hairs appeared to be shifted more towards the apical end in AIP1-2-FP overexpressing seedlings compared to the wild type (Fig. 16A, 16B). These preliminary data suggest that overexpression of AIP1-2 affect root hair positioning by introducing a slight apical shift.

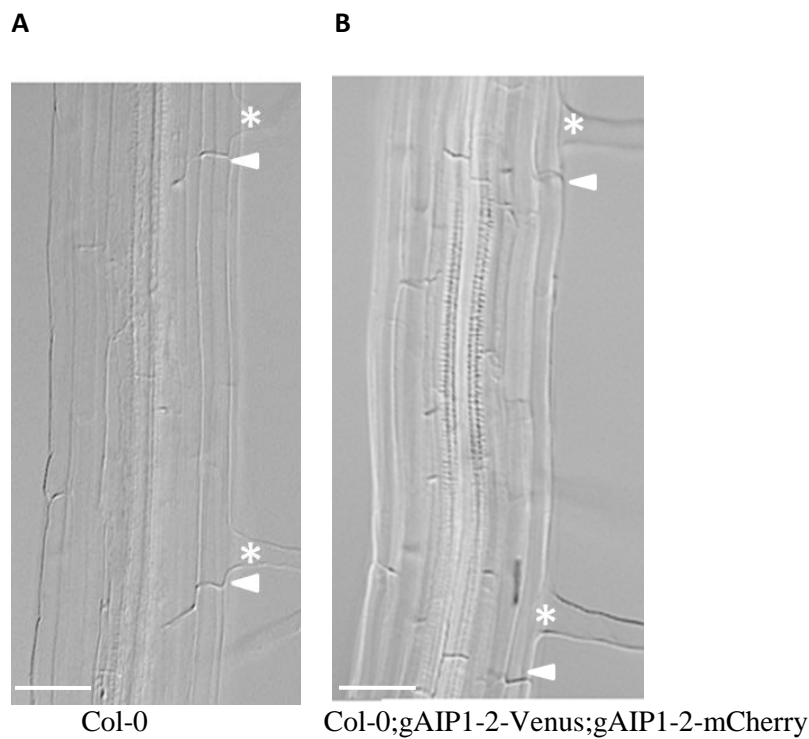


Figure 16. Root hair positioning analysis. Arrowheads show apical and basal end of the cell whereas asterisks show root hair initiation sites. (A) Wild type Col-0. (B) Plant strongly expressing both gAIP1-2-Venus and gAIP1-2-mCherry in Col-0 background that are likely homozygous for both transgenes. Scale bar: 50 μm.

4.3. Specific *AIP-2* promoter activity in hair cells

4.3.1. Generation of promoter-fusion lines

To study the expression pattern of *AIP1-2* in roots, we analyzed the promoter activity of *AIP1-2* by transforming an ER-resident mCherry construct under control of the native *AIP1-2* 5' and 3' genomic regions into *Arabidopsis thaliana* Col-0. Prior to this study, the vector carrying the construct (pGreenII0229-pAIP1-2::ER-mCherry-HDEL::tAIP1-2) had already been transformed into *Agrobacterium tumefaciens* by Christian Kiefer. Here, colony PCR was employed to confirm the presence of the construct in the transformed *Agrobacterium tumefaciens*. Using insert-specific primers, the presence of the transgene was confirmed in *Agrobacterium tumefaciens* as we observed the expected fragment of approximately 814 bp (Fig. 17).

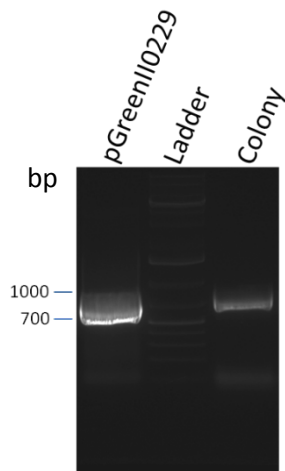
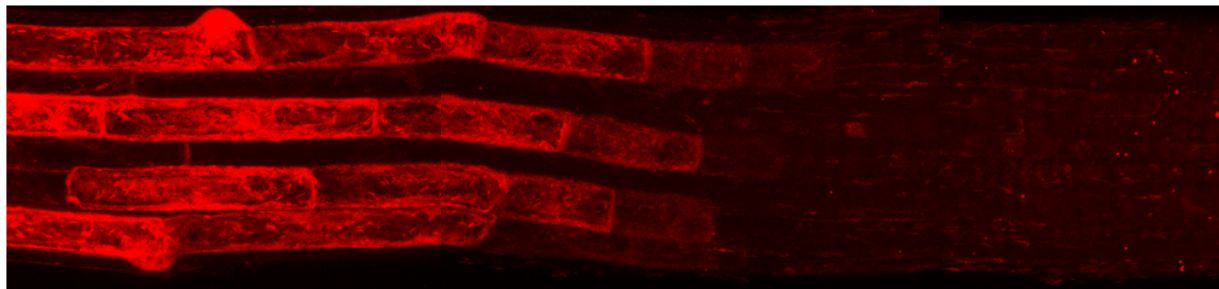


Figure 17. Agarose gel showing results of colony PCR on *Agrobacterium* clones transformed with an ER-resident mCherry construct under control of the native *AIP1-2* genomic region. The purified vector pGreenII 0229 was used as a positive control.

4.3.2. Characterization of promoter-fusion lines

After *Agrobacterium*-mediated transformation, T1-transformant plants were selected using BASTA and T2 plants were analyzed using CSLM. To obtain the optimal settings for analysis of

the expression of the *ER-mCherry-HDEL* reporter, we performed a lambda scan using the 561 nm laser in the spectral region of 446-608 nm (Supplementary Fig. 8.4). Considering the relative increase of background above 652 nm wavelength, as observed by the lambda scan acquired using the same laser settings on the wild type control plants (Supplementary Fig. 8.9), the emission spectrum for detection of ER-mCherry-HDEL fluorescence was set to 569-647 nm. These settings were used for the further analysis of the *ER-mCherry-HDEL* reporter. Using excitation at 561nm fluorescence was observed from the elongation zone onwards (Fig. 18). Intriguingly, in contrast to functional *gAIP1-2-mCherry* construct, no specific fluorescence was observed in the meristematic region (Fig. 18, Supplementary Fig. 8.7).



Maturation zone

Elongation zone

Meristematic zone

Figure 18. *AIP1-2* promoter activity in roots of five-day-old *Arabidopsis* seedlings. The image shows maximum intensity projections of z-stacks acquired in two consecutive sections of the root and assembled together.

5. Discussion

The aim of this study was to further characterize the interaction between AIP1-2 and ACT2 or ACT7. Furthermore, we analyzed the expression pattern of *AIP1-2* in the root based on its promoter activity, and the planar polarity of root hair positioning when AIP1-2 is overexpressed. Our data revealed that AIP1-2 interacts with ACT2 and ACT7. *AIP1-2* seems to be preferentially expressed in hair cell files and overexpression of presumably functional AIP1-2 may shift the root hair positioning towards the apical end.

5.1. Protein-protein interaction between AIP1 homologs and actins

AIP1 was first identified by screening actin binding proteins using yeast two-hybrid system (Amberg *et al.*, 1995). Markus Grebe's group has shown a strong genetic interaction between *Arabidopsis* homolog *AIP1-2* and *ACT7* (Kiefer and Grebe, unpublished results). However, it is not known whether *Arabidopsis* AIP1 homologs interact with actins directly at the protein level.

5.1.1. AIP1-1 and AIP1-2 interact with actins from plant extracts

In this study, we showed that both AIP1 homologs from *Arabidopsis* AIP1-1 and AIP1-2 interact with actins from plant extracts using *in vitro* pull-down method. Western blot analysis of cell suspension protein extracts using anti-actin-11 antibody revealed that GST-AIP1-1 and GST-AIP1-2 specifically precipitated actins. The anti-actin-11 antibody did not only recognize bands of actin size, but also protein bands corresponding to the size of GST, GST-AIP1-1 and GST-AIP1-2 (Fig. 9A). To clarify the nature of these bands, we used anti-GST antibody. This revealed that those bands on the anti-actin-11 blot most likely represented the GST proteins, and that the signal was unspecific probably due to a high amount of GST proteins on the membrane (Fig. 9B, 9C). Taken together, these findings demonstrated that AIP1-1 and AIP1-2 interact with actins from plant extracts at the protein level.

In different organisms, mutation or partial loss of function of AIP1 has been linked to defects in actin organization (Augustine *et al.*, 2011; Ren *et al.*, 2007; Rodal *et al.*, 1999). *Arabidopsis* AIP1 RNAi lines display thick actin bundles compared to wild type suggesting a decrease of actin depolymerization (Ketelaar *et al.*, 2004). In addition, when AIP1-1 is overexpressed, actin organization is disrupted with unusual appearance of thinner actin bundles suggesting a high depolymerization activity (Ketelaar *et al.*, 2007). Therefore, our data suggest that the observed interaction between actins and AIP1-1 or AIP1-2 may be important for actin depolymerization which is essential for actin organization.

Previous studies showed that AIP1-1 is primarily expressed in reproductive tissues whereas AIP1-2 is expressed in both reproductive and vegetative tissues (Allwood *et al.*, 2002). In addition, actin isoforms are predominantly expressed in vegetative or reproductive tissues (Fig. 4A) (Kandasamy *et al.*, 2009). In our study, the specific actin isoforms pulled down from plant extracts are not known. It is interesting to know which actin isoform is pulled down by AIP1-1 or AIP1-2 to analyze whether there is a specificity between AIPs and actin isoforms. Unspecificity in the interaction between AIPs and actin isoforms will suggest that the distinct developmental roles of the AIP1s are mediated by differential gene expression rather than differential specificities for interacting partners. Furthermore, analysis of *aip1-1* and *aip1-2* mutants as well as *aip1-1;aip1-2* double mutants could shed light on whether *Arabidopsis* AIP1 homologs have specific or redundant functions.

5.1.2. His-ACT2 and His-ACT7 expression in Rosetta (DE3) cells.

Expression of recombinant actin in *E. coli* presents several difficulties. One example is the reduced solubility of actin due to actin polymerization occurring during cell lysis or protein purification. In addition, lack of eukaryotic chaperonins in *E. coli* may result in proteins that are not properly folded (Tamura, *et al.*, 2011). Moreover, Shine-Dalgarno sequences within the coding region of actin can potentially induce expression of short regions leading to insoluble aggregates (Frankel, *et al.*, 1990). To facilitate the expression of proteins which show such difficulties, an expression system based on the pCold I vector has been developed (Qing, *et al.*,

2004). To prevent depolymerization and thus insolubility, the buffers to be used during purification processes need ADP rather than ATP, high pH and low salt concentration (Tab. 1) (Oda *et al.*, 2001; Tamura, *et al.*, 2011).

We demonstrated that His-ACT2 and His-ACT7 can be expressed in *E. coli* using the pCold I vector system, similarly to what was shown previously for production of recombinant human β -actin (Tamura, *et al.*, 2011). Analysis of the bacterial protein extracts using the Coomassie staining protocol, showed a band of His-ACT2 or His-ACT7 for bacteria expressing His-ACT2 or His-ACT7 but not in bacteria transformed with empty pCold I vector (Fig. 10C). Consistent with the notion that expression of soluble recombinant actin in bacteria proved difficult for other groups, a large fraction of both His-ACT2 and His-ACT7 was insoluble (Supplementary Fig. 8.1). Further expression analysis using anti-actin-11 antibody on a western blot, revealed actin protein in bacteria expressing His-ACT2 and His-ACT7 (Fig. 10A). Anti-His antibody probing after stripping the membrane also revealed the presence of His-ACT2 and His-ACT7 in bacteria expressing His-ACT2 and His-ACT7 (Fig. 10B). These results demonstrated that soluble recombinant *Arabidopsis* actins can be expressed in *E. coli* although to a low extent.

To my knowledge, this is the first time that an actin from a plant species has been recombinantly expressed in bacteria. This will help future *in vitro* studies to examine interaction of specific actin isoforms and actin-interacting proteins. Importantly, in our study, studying interaction of bacterially expressed actin isoform and AIP1 homologs excludes the possibility that eukaryotic proteins such as ADF mediate this interaction in our assay.

5.1.3. AIP-2 interacts with ACT7

We found that GST-AIP1-2 interacts with His-ACT7 in an *in vitro* pull-down experiment. Western blot analysis using anti-actin-11 antibody revealed that GST-AIP1-2 pulled down bacterially expressed His-ACT7 in contrast to all controls (Fig. 11A). Thus, this data demonstrated that GST-AIP1-2 specifically precipitated bacterially expressed His-ACT7,

implying that ADF or other eukaryotic proteins are not needed for interaction of AIP-2 and ACT7.

It has been shown that AIP1-2 interacts with ACT7 using yeast two-hybrid system (Claes, Kiefer and Grebe, unpublished results). One of the disadvantages of the yeast two-hybrid system is that endogenously expressed yeast ADF/cofilin or other yeast specific components could mediate this interaction. Since the GST-AIP1-2 and His-ACT7 fusion proteins used in our study were recombinantly expressed in *E. coli*, which does not contain any close homologs of the eukaryotic actin machinery, it is likely that the interaction observed between AIP1-2 and ACT7 is direct. To further confirm our data, it will be interesting to attempt to further purify His-ACT7 via the His tag for example using nickel nitrilotriacetic acid (NiNTA) resin and to attempt to pull it down with purified GST-AIP1-2.

AIP1-2 has been shown to interact genetically with ACT7 (Kiefer and Grebe, unpublished results). While *act7* mutants display aberrant plant development and *aip1-2* mutants show almost the wild type phenotype, *act7;aip1-2* mutants present a very strong reduced germination compared to single mutants, pointing out a strong synergistic genetic interaction between these two genes *in vivo*. The fact that we observed interaction between AIP1-2 and ACT7 suggests that these two proteins not only interact genetically *in vivo* but also at the protein level.

ACT7 has been implicated in root hair initiation (Kandasamy *et al.*, 2009). This is because *act7* mutants display a reduced root hair density whereas root hair length is normal (Kandasamy *et al.*, 2009). Furthermore, *act7* mutants display an apical shift of root hair positioning compared to the wild type indicating its role in planar polarity of root hairs (Ikeda and Grebe, unpublished results). AIP1-2 is also involved in planar polarity of root hairs since *aip1-2* mutants display a basal shift of root hair positioning compared to the wild type (Claes, Kiefer and Grebe, unpublished results). Considering the defect of *act7* mutants in root hair initiation and root hair positioning, and the defect of *aip1-2* mutants in root hair positioning, our results suggest that interaction of ACT7 and AIP1-2 is important for root hair positioning and root hair initiation.

5.1.4. AIP-2 interacts with ACT2

Our study showed an interaction between AIP1-2 and ACT2 in an *in vitro* pull-down experiment. Western blot analysis using anti-actin-11 antibody showed that GST-AIP1-2 precipitated bacterially expressed ACT2 (Fig. 12A). The bead and GST incubated with extracts of bacteria expressing ACT2 retained a small amount of actin (Fig. 12A). The increase in background label in this experiment compared to previous experiments presumably depends on the higher amount of GST on the beads, as revealed by Coomassie stained gel and Western blot using anti-GST antibody (Fig. 12B, 12C). This background can be neglected due to the fact that it is much less compared to the amount of actin precipitated by GST-AIP1-2 (Fig. 12A, 12C). An additional washing step after incubating different beads (pure bead, bead linked to GST, bead linked to GST-AIP1-2) with bacteria extracts (see 3.6.2) may also eliminate the bead background. Additional bands observed for GST-AIP1-2 seems to be degradation of this fusion protein that probably led to a very lower amount GST-AIP1-2 than GST alone (Fig. 12B). Taken together, our data showed interaction between AIP1-2 and ACT2 expressed in bacteria, indicating that no eukaryotic proteins such as ADF mediate this interaction. Similar to ACT7 pull down experiment in this study, future works to confirm our results could be employing His-ACT2 purified via His tag in order to pull down purified GST-AIP1-2.

ACT2 has been shown to participate in root hair initiation and root elongation because *act2* mutants present defects in bulge formation and shorter root hairs compared to the wild type (Ringli *et al.*, 2002). In addition, *act2* mutants display an apical shift of root hair formation meaning that ACT2 is involved in planar polarity of root hair formation (Ikeda and Grebe, unpublished results). Based on the *act2* mutants defect in root hair positioning and root hair formation together with *aip1-2* mutants defect in root hair positioning (Claes, Kiefer and Grebe, unpublished results), our results support the view that direct interaction between ACT2 and AIP1-2 is important for planar polarity, for the initiation and for the elongation of root hairs.

5.2. Overexpression of AIP1-2 may lead to an apical shift of root hair positioning

Downregulation and overexpression of *Arabidopsis* AIP1 homologs interfere with actin organization suggesting a defect of actin depolymerization function (Ketelaar *et al.*, 2004, Ketelaar *et al.*, 2007). Although *Arabidopsis* AIP1s seem to be important for root hair formation and overall in plant development (Ketelaar *et al.*, 2004; Ketelaar *et al.*, 2007), no single mutant had been characterized. Previous work in Markus Grebe's group revealed that *aip1.2* mutants display a significant basal shift of root hair positioning compared to the wild type, suggesting a role of AIP1-2 in planar polarity establishment (Claes, Kiefer and Grebe, unpublished results). However, AIP1-2 function in planar polarity establishment is not well understood.

To further investigate the role of AIP1-2 during establishment of planar root hair polarity, we generated AIP1-2 overexpressing lines carrying four or more copies of a presumably functional *AIP1-2* gene. Western blot analysis of protein extracts using anti-RFP and anti-GFP antibody as well as CLSM analysis revealed that selected T2 lines that had been crossed each other were expressing gAIP1-2-mCherry or gAIP1-2-Venus (Fig. 14, 15A, 15B). Analysis of transgene expression in AIP1-2 overexpressing lines using CLSM confirmed the expression of both gAIP1-2-mCherry and gAIP1-2-Venus in these lines (Fig. 15C). We analyzed root hair positioning of AIP1-2 overexpressing lines only in a few seedlings due to a limited time of this study. In these seedlings root hairs appeared to be shifted apically compared to the wild type (Fig. 16A, 16B). Hence, our preliminary studies suggest that AIP1-2 overexpression may result in an apical shift of root hair positioning.

The fact that *aip1.2* mutants display a basal shift (Ikeda, Claes, Kiefer and Grebe, unpublished results) while AIP1-2 overexpressing lines tentatively display an apical shift suggests that AIP1-2 may have a regulatory role in polar root hair positioning. In this study, we showed that AIP1-2 can interact with ACT2 and ACT7. It has been shown that *act2* and *act7* mutants display apical shifts of root hair positioning (Ikeda and Grebe, unpublished results). Thus, our data that AIP1-2 appears to shift root hairs apically is consistent with the idea that AIP1-2 may regulate ACT2 and ACT7 in planar polarity of root hairs. Future studies could address whether mutation or overexpression of ADF can mimic the root hair phenotype of *aip1-2* mutants and AIP1-2

overexpression respectively. Overexpressing AIP1-2 together with an ADF isoform that is preferentially expressed in root hair cells may also show AIP1-2 involvement in root hair positioning. In our study, endogenous AIP1-2 protein may be downregulated in the generated AIP1-2 overexpressing lines. To examine this scenario, Western blot analysis using anti-AIP1 antibody could be employed for AIP1-2 overexpressing lines, and parental lines that were crossed each other.

5.3. *AIP1-2* appears to be preferentially expressed in hair cell files

Different genes involved in *Arabidopsis* root hair patterning can be preferentially expressed in hair or non-hair cell files (Schiefelbein *et al.*, 2009). Previous studies showed that AIP1-2-mCherry protein expressed under the control of the *AIP1-2* genomic region is preferentially enriched in hair cell files (Kiefer and Grebe, unpublished). This raises the question whether the *AIP1-2* promoter is specifically active in hair cell files, or whether it is active in non-hair cell files as well, and whether AIP1-2 later moves to hair cell files or gets degraded in non-hair cells.

Here we showed that *AIP1-2* promoter activity appears to be preferentially restricted to hair cell files. Using CLSM analysis of the *AIP1-2* promoter activity by employing an ER-resident mCherry construct cloned under the control of the native *AIP1-2* genomic region, fluorescence was observed preferentially in hair cell files (Fig. 18) from the elongation zone onwards. It is interesting to note that the previously observed expression of a genomic *AIP1-2* construct fused to mCherry in the meristematic zone (Fig. 18, Supplementary Fig. 8.7) was not observed for the promoter fusion construct used in this study. The promoter activity of a gene does not necessarily reflect the expression of the gene because it may be regulated at the mRNA or at the protein level. However, our results suggest that *AIP1-2* is preferentially expressed specifically in hair cell files of the epidermis, less in the meristematic region even below the detection level of our method. Considering the previously observed presence of AIP1-2 protein in the meristem, together with the apparent absence of *AIP1-2* promoter activity in this region, this raises the question how the protein gets localized there. One idea that is supported by the data provided here is that AIP1-2 expressed in hair cell files may move into the meristematic region. A double

or triple GFP-tagged version that prevents cell-to-cell movement may be used for AIP1-2 to further test this hypothesis of AIP1-2 movement to the meristematic region (Kurata *et al.*, 2005).

The designation of root epidermal cell fate is accomplished by a complex of genes that are expressed preferentially in hair or non-hair cell files (Schiefelbein *et al.*, 2009). For example *WEREWOLF* (*WER*), the main regulator of root hair patterning is expressed preferentially in non-hair cells and is involved in specification of both hair and non-hair cell fate (Schiefelbein *et al.*, 2009). *GL2* is another gene expressed in non-hair cell files, which participates in non-hair cell fate specification (Lin and Aoyama, 2012). Analysis of root hair patterning in *aip1-2* mutants may show whether AIP1-2 is also involved in patterning. Since *WER* regulates different genes that are involved in root hair patterning, analysis of AIP1-2 expression pattern in *wer* mutant will indicate whether AIP1-2 expression is regulated by *WER*.

5.4. Conclusions and perspectives

In this study, we showed that AIP1-1 and AIP1-2 interact with actins from plant extracts. Future work will help to identify the specificity between *Arabidopsis AIP1* homologues and actin isoforms. Analysis of *aip1-1* and *aip1-2* single mutants and *aip1-1;aip1-2* mutants may show whether AIP1-1 and AIP1-2 display specificity towards different actin isoforms or act redundantly. Our findings showed that His-ACT2 and His-ACT7 can be expressed in *E. coli*. This may aid *in vitro* studies that would rely on actin production in bacteria. For future studies requiring a high amount of actin, different steps of actin purification would need to be optimized. These could include cell lysis, since it largely affects protein solubility, and preparation of buffer that has to depend on the specific properties of actin. Our data revealed interaction between AIP1-2 and bacterially expressed ACT2 or ACT7, indicating that other eukaryotic proteins are not required for this interaction in our assay. Purification of ACT2 or ACT7 to pull down AIP1-2 may help to further confirm these results. Although it is too early to draw conclusions based on statistically significant data, our results suggest that AIP1-2 overexpression may lead to an apical shift of root hair positioning. Quantification of this apical shift phenotype will be important. Based on AIP1-2 promoter activity, our data suggest that AIP1-2 is predominantly expressed in

hair cell files from elongation zone onwards. Since the promoter activity analysis suggests that AIP1-2 is not expressed in meristematic region but may move to this region, a double or triple GFP-tag that hinders cell-to-cell movement may provide evidence for this hypothesis.

6. Acknowledgements

I would like to offer my special thanks to Prof. Dr. Markus Grebe for giving me the opportunity to work in his group as well as for providing me this project and his supervision with useful critiques.

I wish to thank Christian Kiefer, my co-supervisor, for teaching me several things in the laboratory, his comments on the manuscript and his constant encouragement.

I would also like to extend my thanks to Prof. Dr. Markus Grebe group members and all the people in the UPSC for their assistance during my laboratory work.

Lastly but not the least, I thank the Swedish Institute (SI) for financially supporting my studies of Masters program.

7. References

- Allwood EG, Anthony RG, Smertenko AP, Reichelt S, Drobak BK, Doonan JH, Weeds AG, Hussey PJ (2002) Regulation of the pollen-specific actin-depolymerizing factor LIADF1. *Plant Cell* 14: 2915-2927
- Alonso JM, Hirayama T, Roman G, Nourizadeh S, Ecker JR (1999) EIN2, a bifunctional transducer of ethylene and stress responses in *Arabidopsis*. *Science* (New York, NY) 284: 2148-2152
- Amberg DC, Basart E, Botstein D (1995) Defining protein interactions with yeast actin in-vivo. *Nature Structural Biology* 2: 28-35
- Apte, A., and Daniel, S. (2009). PCR primer design. *Cold Spring Harbor Protocols*; doi:10.1101/pdb.ip65
- Augustine RC, Pattavina KA, Tuzel E, Vidali L, Bezanilla M (2011) Actin interacting protein1 and actin depolymerizing factor drive rapid actin dynamics in *Physcomitrella patens*. *Plant Cell* 23: 3696-3710
- Berger F, Haseloff J, Schiefelbein J, Dolan L (1998) Positional information in root epidermis is defined during embryogenesis and acts in domains with strict boundaries. *Current Biology* 8: 421-430
- Blair A, Tomlinson A, Pham H, Gunsalus KC, Goldberg ML, Laski FA (2006) Twinstar, the *Drosophila* homolog of cofilin/ADF, is required for planar cell polarity patterning. *Development* 133: 1789-1797
- Cramer L (2008) Organelle Transport: Dynamic Actin Tracks for Myosin Motors. *Current Biology* 18: R1066-R1068
- Dolan L, Costa S (2001) Evolution and genetics of root hair stripes in the root epidermis. *Journal of Experimental Botany* 52: 413-417

Dolan L, Duckett CM, Grierson C, Linstead P, Schneider K, Lawson E, Dean C, Poethig S, Roberts K (1994) Clonal relationships and cell patterning in the root epidermis of *Arabidopsis*. *Development* 120: 2465-2474

Eaton S, Wepf R, Simons K (1996) Roles for Rac1 and Cdc42 in planar polarization and hair outgrowth in the wing of *Drosophila*. *Journal of Cell Biology* 135: 1277-1289

Einarson MB, Pugacheva EN, Orlinick JR (2007) Identification of Protein-Protein Interactions with Glutathione-S-Transferase (GST) Fusion Proteins. *CSH protocols*: pdb.top11

Fine, A. (2007) Confocal microscopy: principles and practice. *CSH Protoc*, pdb.top22.

Fischer U, Ikeda Y, Ljung K, Serralbo O, Singh M, Heidstra R, Palme K, Scheres B, Grebe M (2006) Vectorial information for *Arabidopsis* planar polarity is mediated by combined AUX1, EIN2, and GNOM activity. *Current biology*: CB 16: 2143-2149

Frankel, S., Condeelis, J., and Leinwand, L. (1990). Expression of actin in *Escherichia coli*. Aggregation, solubilization, and functional analysis. *J Biol Chem* 265, 17980-17987.

Friml J, Vieten A, Sauer M, Weijers D, Schwarz H, Hamann T, Offringa R, Jurgens G (2003) Efflux-dependent auxin gradients establish the apical-basal axis of *Arabidopsis*. *Nature* 426: 147-153

Fu Y, Yang Z (2001a) Rop GTPase: a master switch of cell polarity development in plants. *Trends in plant science* 6: 545-547

Grebe M (2004) Ups and downs of tissue and planar polarity in plants. *BioEssays: news and reviews in molecular, cellular and developmental biology* 26: 719-729

Grebe M, Friml J, Swarup R, Ljung K, Sandberg G, Terlou M, Palme K, Bennett MJ, Scheres B (2002) Cell polarity signaling in *Arabidopsis* involves a BFA-sensitive auxin influx pathway. *Current biology*: CB 12: 329-334

Grebe M, Xu J, Scheres B (2001) Cell axiality and polarity in plants-adding pieces to the puzzle. *Current opinion in plant biology* 4: 520-526

Harlow, E., and Lane, D. (2006). *Cold Spring Harb Protoc*; doi:10.1101/pdb.prot4644.

Hussey P. (2004) Actin and actin modulating proteins. P. Hussey (Ed), The Plant Cytoskeleton in Cell Differentiation and Development, Blackwell: Oxford, 265-289

Iida K, Yahara I (1999) Cooperation of two actin-binding proteins, cofilin and Aip1, in *Saccharomyces cerevisiae*. *Genes to cells: devoted to molecular & cellular mechanisms* 4: 21-32

Ikeda Y, Men S, Fischer U, Stepanova AN, Alonso JM, Ljung K, Grebe M (2009) Local auxin biosynthesis modulates gradient-directed planar polarity in *Arabidopsis*. *Nature cell biology* 11: 731-738

Jones MA, Shen JJ, Fu Y, Li H, Yang ZB, Grierson CS (2002) The *Arabidopsis* Rop2 GTPase is a positive regulator of both root hair initiation and tip growth. *Plant Cell* 14: 763-776

Kandasamy MK, Burgos-Rivera B, McKinney EC, Ruzicka DR, Meagher RB (2007) Class-specific interaction of profilin and ADF isoforms with actin in the regulation of plant development. *Plant Cell* 19: 3111-3126

Kandasamy MK, McKinney EC, Meagher RB (2009) A single vegetative actin isoform overexpressed under the control of multiple regulatory sequences is sufficient for normal *Arabidopsis* development. *Plant Cell* 21: 701-718

Ketelaar T, Allwood EG, Anthony R, Voigt B, Menzel D, Hussey PJ (2004) The actin-interacting protein AIP1 is essential for actin organization and plant development. *Current Biology* 14: 145-149

Ketelaar T, Allwood EG, Hussey PJ (2007) Actin organization and root hair development are disrupted by ethanol-induced overexpression of *Arabidopsis* actin interacting protein 1 (AIP1). *New Phytologist* 174: 57-62

Kleine-Vehn J, Dhonukshe P, Sauer M, Brewer PB, Wiśniewska J, Paciorek T, Benková E, Friml J (2008) ARF GEF-Dependent Transcytosis and Polar Delivery of PIN Auxin Carriers in Arabidopsis. *Current Biology* 18: 526-531

Kleine-Vehn J, Friml J (2008) Polar targeting and endocytic recycling in auxin-dependent plant development. *Annual review of cell and developmental biology* 24: 447-473

Kurata T, Ishida T, Kawabata-Awai C, Noguchi M, Hattori S, Sano R, Nagasaka R, Tominaga R, Koshino-Kimura Y, Kato T, Sato S, Tabata S, Okada K, Wada T (2005) Cell-to-cell movement of the CAPRICE protein in Arabidopsis root epidermal cell differentiation. *Development* 132: 5387-5398

Le Clainche C, Carlier MF (2008) Regulation of actin assembly associated with protrusion and adhesion in cell migration. *Physiological Reviews* 88: 489-513

Lew DJ (2002) Formin actin filament bundles. *Nature cell biology* 4: E29-E30

Li R, Gundersen GG (2008) Beyond polymer polarity: how the cytoskeleton builds a polarized cell. *Nature reviews Molecular cell biology* 9: 860-873

Lin Q, Aoyama T (2012) Pathways for epidermal cell differentiation via the homeobox gene *GLABRA2*: update on the roles of the classic regulator. *Journal of integrative plant biology* 54: 729-737

Liu PW, Qi M, Xue XH, Ren HY (2011) Dynamics and functions of the actin cytoskeleton during the plant cell cycle. *Chinese Science Bulletin* 56: 3504-3510

Macara IG, Mili S (2008) Polarity and Differential Inheritance Universal Attributes of Life? *Cell* 135: 801-812

Marchant A, Kargul J, May ST, Muller P, Delbarre A, Perrot-Rechenmann C, Bennett MJ (1999) *AUX1* regulates root gravitropism in *Arabidopsis* by facilitating auxin uptake within root apical tissues. *Embo j* 18: 2066-2073

Marcinkevicius E, Fernandez-Gonzalez R, Zallen JA (2009) Q&A: quantitative approaches to planar polarity and tissue organization. *J Biol* 8: 103

Masucci JD, Schiefelbein JW (1994) The *rh6* Mutation of *Arabidopsis thaliana* Alters Root-Hair Initiation through an Auxin-and Ethylene-Associated Process. *Plant physiology* 106: 1335-1346

Mayer U, Buttner G, Jurgens G (1993) Apical-basal pattern-formation in the *Arabidopsis* embryo-studies on the role of the *gnom* gene. *Development* 117: 149-162

Mayer U, Ruiz RAT, Berleth T, Misera S, Jurgens G (1991) Mutations affecting body organization in the *Arabidopsis* embryo. *Nature* 353: 402-407

Mohri K, Ono S (2003) Actin filament disassembling activity of *Caenorhabditis elegans* actin-interacting protein 1 (UNC-78) is dependent on filament binding by a specific ADF/cofilin isoform. *J Cell Sci* 116: 4107-4118

Mohri K, Vorobiev S, Fedorov AA, Almo SC, Ono S (2004) Identification of functional residues on *Caenorhabditis elegans* actin-interacting protein 1 (UNC-78) for disassembly of actin depolymerizing factor/cofilin-bound actin filaments. *The Journal of biological chemistry* 279: 31697-31707

Moseley JB, Goode BL (2006) The yeast actin cytoskeleton: From cellular function to biochemical mechanism. *Microbiology and Molecular Biology Reviews* 70: 605

Oda T, Makino K, Yamashita I, Namba K, Maeda Y (2001) Distinct structural changes detected by X-ray fiber diffraction in stabilization of F-actin by lowering pH and increasing ionic strength. *Biophys J* 80: 841-851

Okada K, Blanchoin L, Abe H, Chen H, Pollard TD, Bamburg JR (2002) *Xenopus* actin-interacting protein 1 (XAip1) enhances cofilin fragmentation of filaments by capping filament ends. *The Journal of biological chemistry* 277: 43011-43016

Ono S (2003) Regulation of actin filament dynamics by actin depolymerizing factor/cofilin and actin-interacting protein 1: new blades for twisted filaments. *Biochemistry* 42: 13363-13370

Ono S (2007) Mechanism of depolymerization and severing of actin filaments and its significance in cytoskeletal dynamics. *International review of cytology* 258: 1-82

Ono S, Mohri K, Ono K (2004) Microscopic evidence that actin-interacting protein 1 actively disassembles actin-depolymerizing factor/cofilin-bound actin filaments. *Journal of Biological Chemistry* 279: 14207-14212

Pollard TD, Cooper JA (2009) Actin, a Central Player in Cell Shape and Movement. *Science* 326: 1208-1212

Qing, G., Ma, L.C., Khorchid, A., Swapna, G.V., Mal, T.K., Takayama, M.M., Xia, B., Phadtare, S., Ke, H., Acton, T., et al. (2004). Cold-shock induced high-yield protein production in *Escherichia coli*. *Nat Biotechnol* 22, 877-882

Ren N, Charlton J, Adler PN (2007) The flare gene, which encodes the AIP1 protein of *Drosophila*, functions to regulate F-actin disassembly in pupal epidermal cells. *Genetics* 176: 2223-2234

Ridge RW (1995) Recent developments in the cell and molecular biology of root hairs. *Journal of Plant Research* 108: 399-405

Ringli C, Baumberger N, Diet A, Frey B, Keller B (2002) ACTIN2 is essential for bulge site selection and tip growth during root hair development of *Arabidopsis*. *Plant physiology* 129: 1464-1472

Rodal AA, Tetreault JW, Lappalainen P, Drubin DG, Amberg DC (1999) Aip1p interacts with cofilin to disassemble actin filaments. *The Journal of cell biology* 145: 1251-1264

Sachs T: The polarization of tissues. In *Pattern Formation in Plant Tissues*. Edited by Sachs T. Cambridge University Press; 1991: 52-69

Sambrook, J., and Russell, D.W. (2006). Detection of DNA in agarose gels. *Cold Spring Harbor Protocols*; doi:10.1101/pdb.prot4022

Sambrook, J., and Russell, D.W. (2006). SDS- Polyacrylamide Gel Electrophoresis of Proteins. *Cold Spring Harbor Protocols*; doi:10.1101/pdb.prot4540

Schiefelbein J, Kwak SH, Wieckowski Y, Barron C, Bruex A (2009) The gene regulatory network for root epidermal cell-type pattern formation in *Arabidopsis*. *J Exp Bot* 60: 1515-1521

Simpson, R.J. (2007). Staining proteins in gels with coomassie blue. CSH Protoc 2007, pdb.prot4719.

Steinmann T, Geldner N, Grebe M, Mangold S, Jackson CL, Paris S, Galweiler L, Palme K, Jurgens G (1999) Coordinated polar localization of auxin efflux carrier PIN1 by GNOM ARF GEF. Science 286: 316-318

Studier, F.W. (2005). Protein production by auto-induction in high density shaking cultures. Protein Expression and Purification 41: 207-234.

Tamura M, Ito K, Kunihiro S, Yamasaki C, Haragauchi M (2011) Production of human beta-actin and a mutant using a bacterial expression system with a cold shock vector. Protein Expression and Purification 78: 1-5

Thomas C, Strutt D (2012) The roles of the cadherins Fat and Dachshous in planar polarity specification in *Drosophila*. Developmental dynamics: an official publication of the American Association of Anatomists 241: 27-39

Ueda M, Laux T (2012) The origin of the plant body axis. Current opinion in plant biology 15: 578-584

Van der Honing HS, Emons AM, Ketelaar T (2007) Actin based processes that could determine the cytoplasmic architecture of plant cells. Biochimica et biophysica acta 1773: 604-614

Yang Z (2008) Cell polarity signaling in Arabidopsis. Annual review of cell and developmental biology 24: 551-575

Young ME, Cooper JA, Bridgman PC (2004) Yeast actin patches are networks of branched actin filaments. Journal of Cell Biology 166: 629-635

Zallen JA (2007) Planar Polarity and Tissue Morphogenesis. Cell 129: 1051-1063

8. Supplementary figures

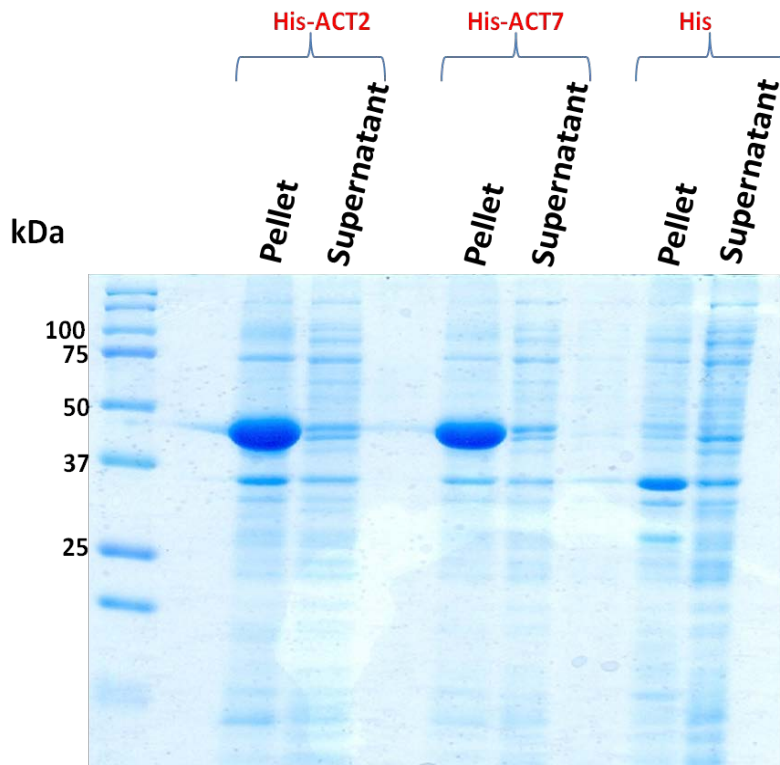


Figure 8.1: Expression of *His-ACT2* and *His-ACT 7* in *E. coli*. Coomassie brilliant blue stained gel showing the presence and approximate amount of bacteria-expressed proteins. The leftmost lane shows the molecular weight markers. Pellet represents proteins from the insoluble fractions after centrifugation of cell lysate, whereas supernatant represents proteins from the soluble fractions. Top label indicates the His-fusion proteins contained in the bacterial extracts.

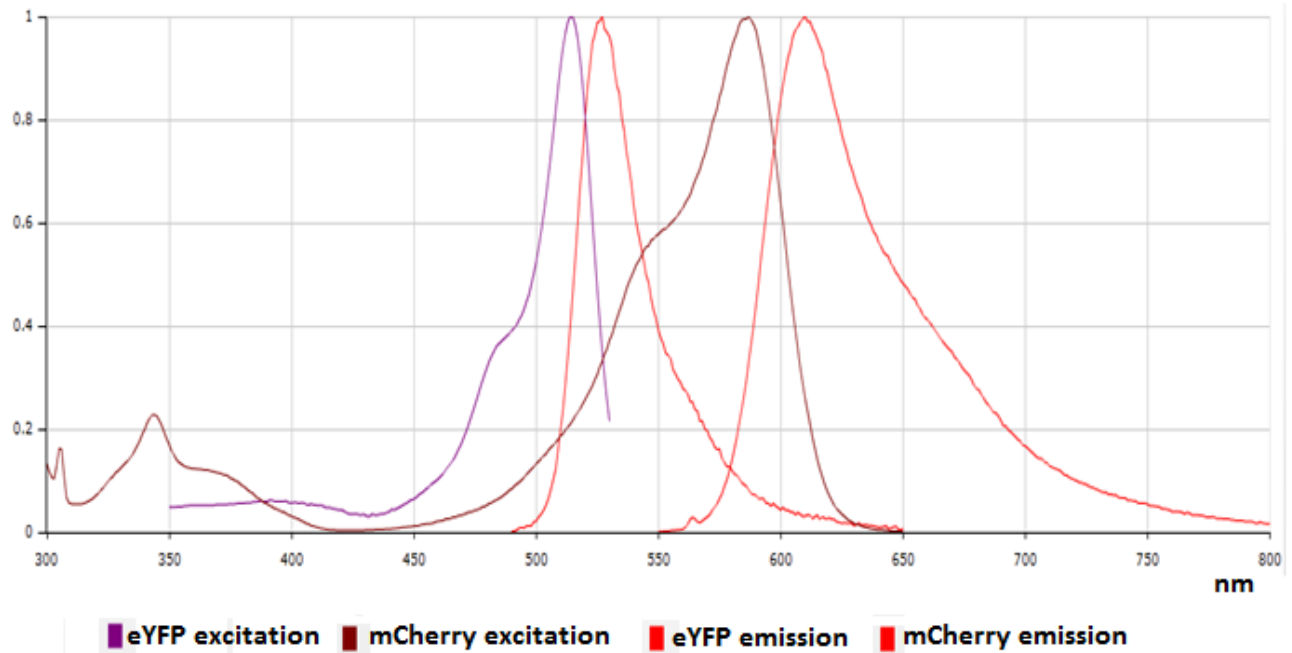


Figure 8.2: Excitation and emission spectra of eYFP and mCherry. Note the overlap of eYFP and mCherry excitation and emission spectra between 500-540 nm, and 550-600 nm, respectively (adapted from <http://www.spectra.arizona.edu>, October. 05. 2013)

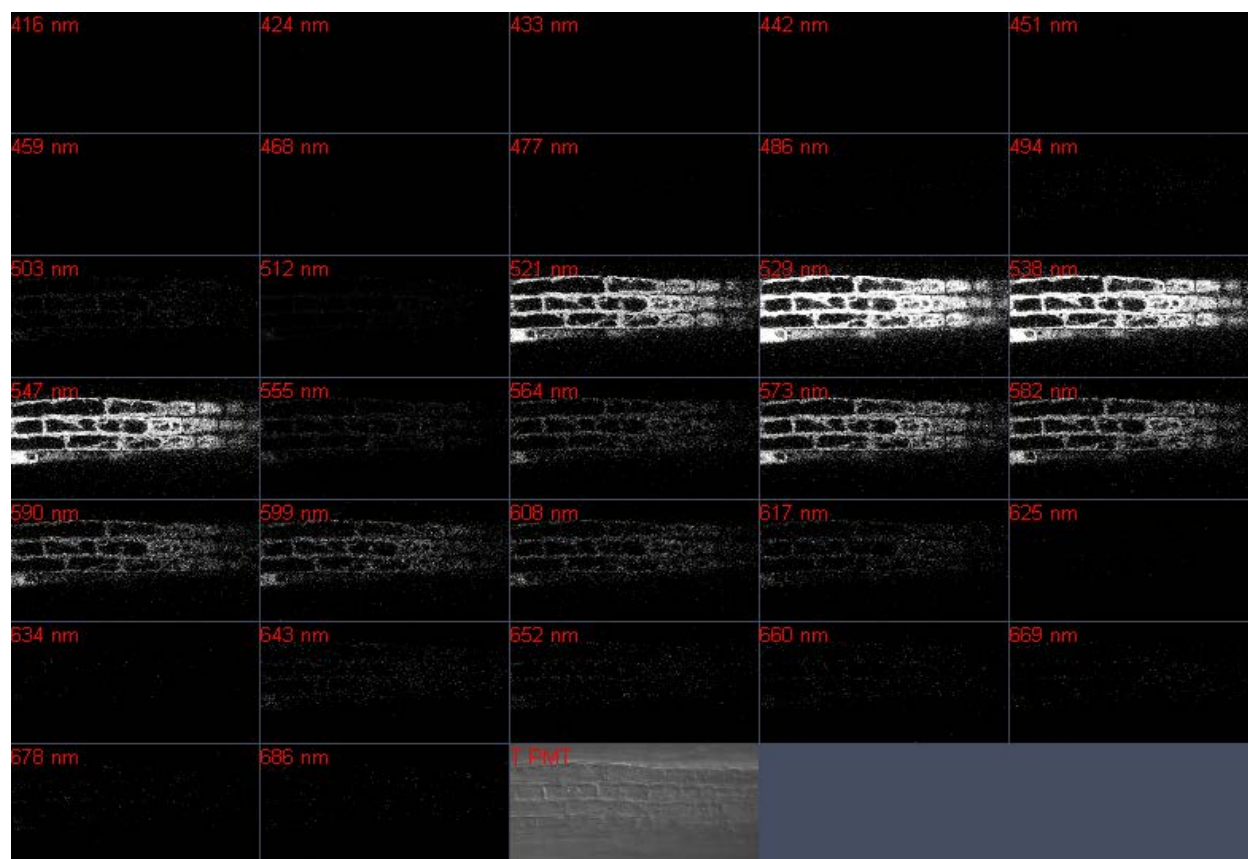


Figure 8.3: Lambda scan analysis in the epidermal layer of the root transition zone of a five-day-old seedling expressing *gAIP1-2-Venus*. Pictures were acquired using the 514 nm laser for excitation and the emission harvested in spectral intervals of 8-9 nm ranging from 416 to 686 nm wavelength. The last picture (T PMT) shows a transmission image.

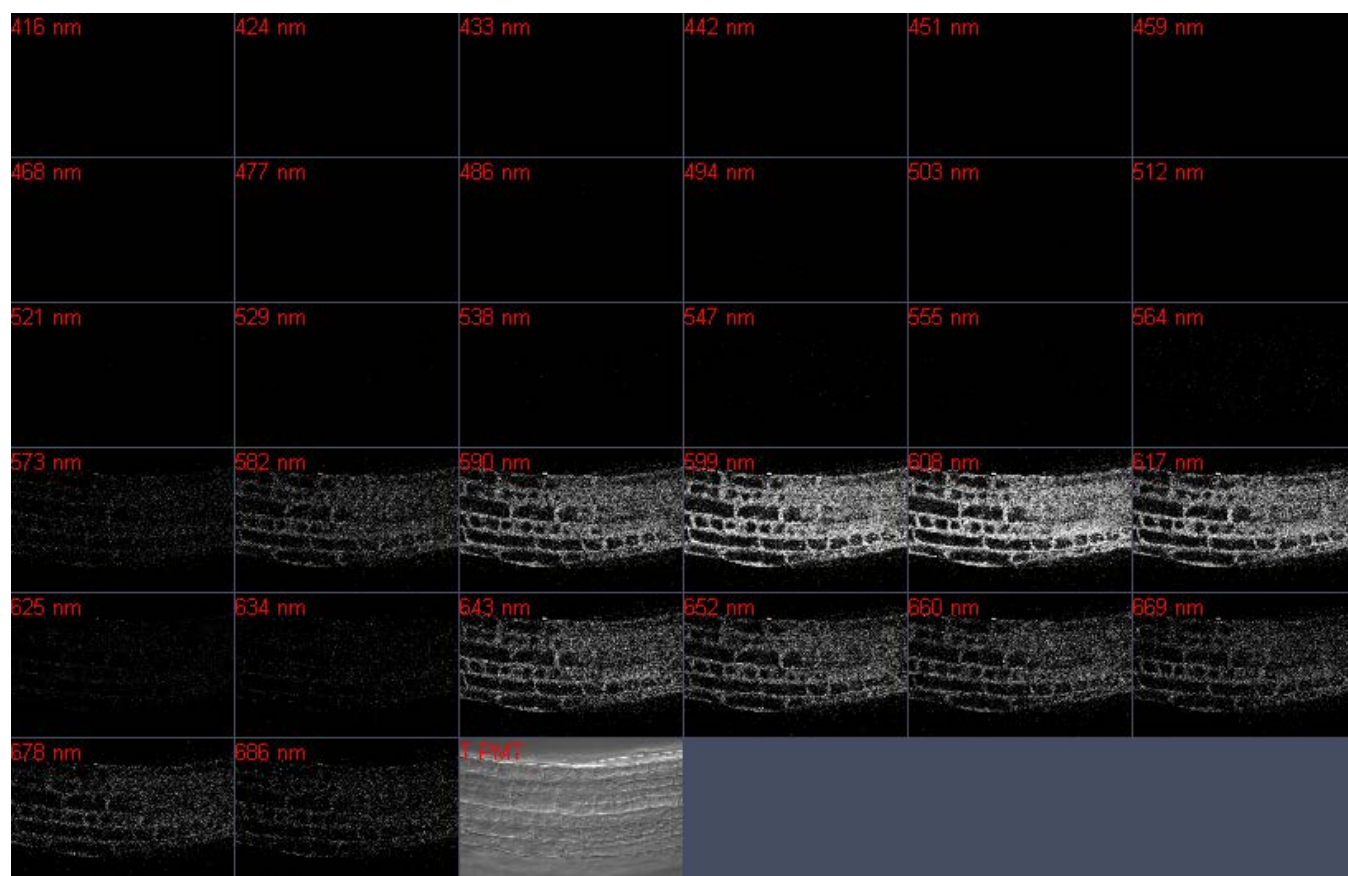


Figure 8.4: Lambda scan analysis in the epidermal layer of the root transition zone of five-day-old seedling expressing *gAIP1-2-mCherry*. Pictures were acquired using the 561 nm laser for excitation and the emission harvested in spectral intervals of 8 – 9 nm ranging from 416 to 686 nm wavelength. The last picture (T PMT) shows a transmission image.

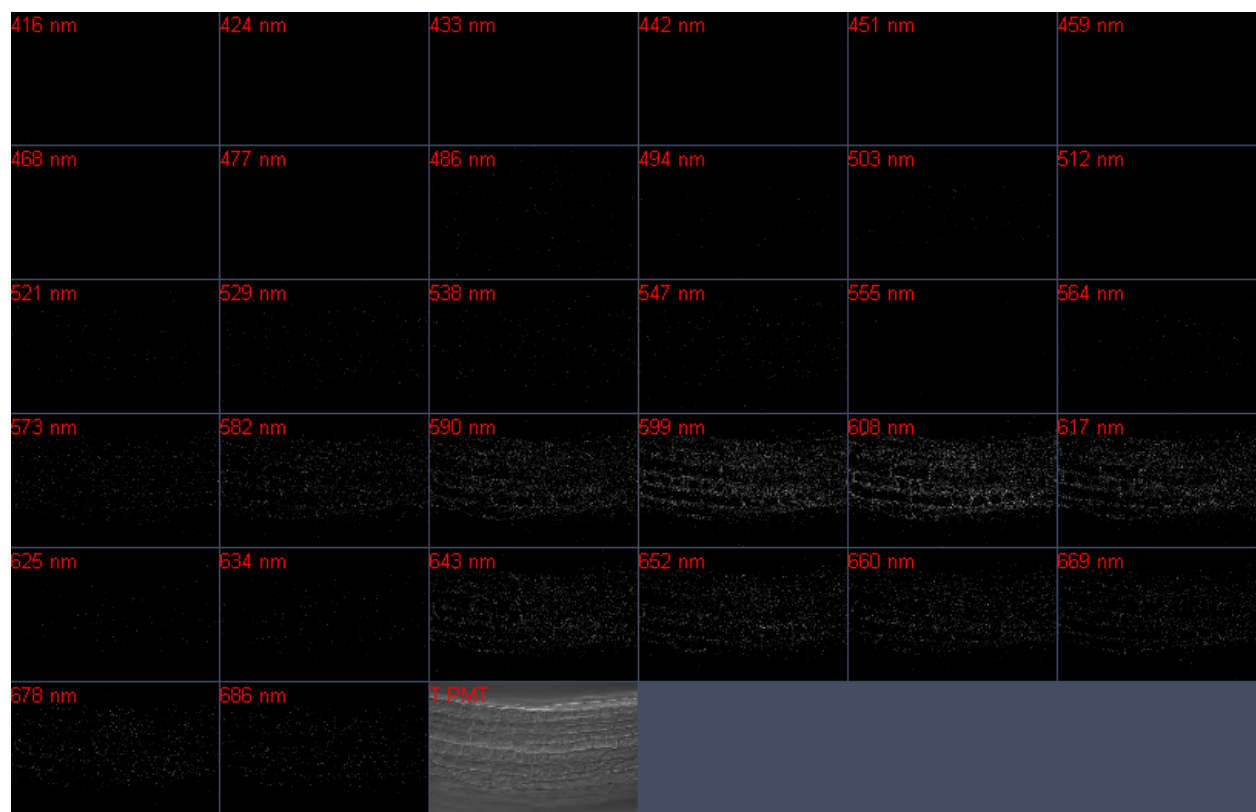


Figure 8.5: Lambda scan analysis in the epidermal layer of the root transition zone of five-day-old seedling expressing *gAIP1-2-mCherry*. Pictures were acquired using the 514 nm laser for excitation and the emission harvested in spectral intervals of 8-9 nm ranging from 416 to 686 nm wavelength. The last picture (T PMT) shows a transmission image.

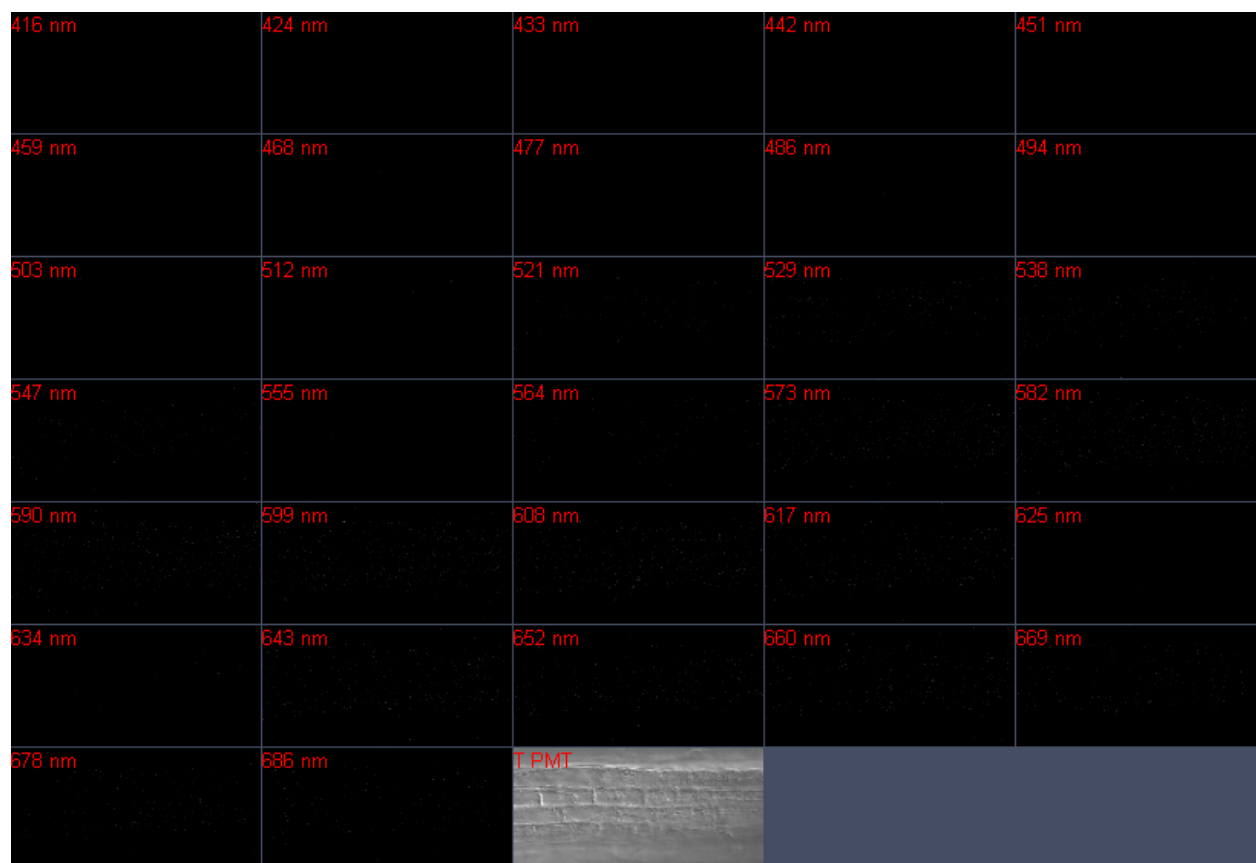


Figure 8.6: Lambda scan analysis in the epidermal layer of the root transition zone of five-day-old seedling expressing *gAIP1-2-Venus*. Pictures were acquired using the 561 nm laser for excitation and the emission harvested in spectral intervals of 8-9 nm ranging from 416 to 686 nm wavelength. The last picture (T PMT) shows a transmission image.

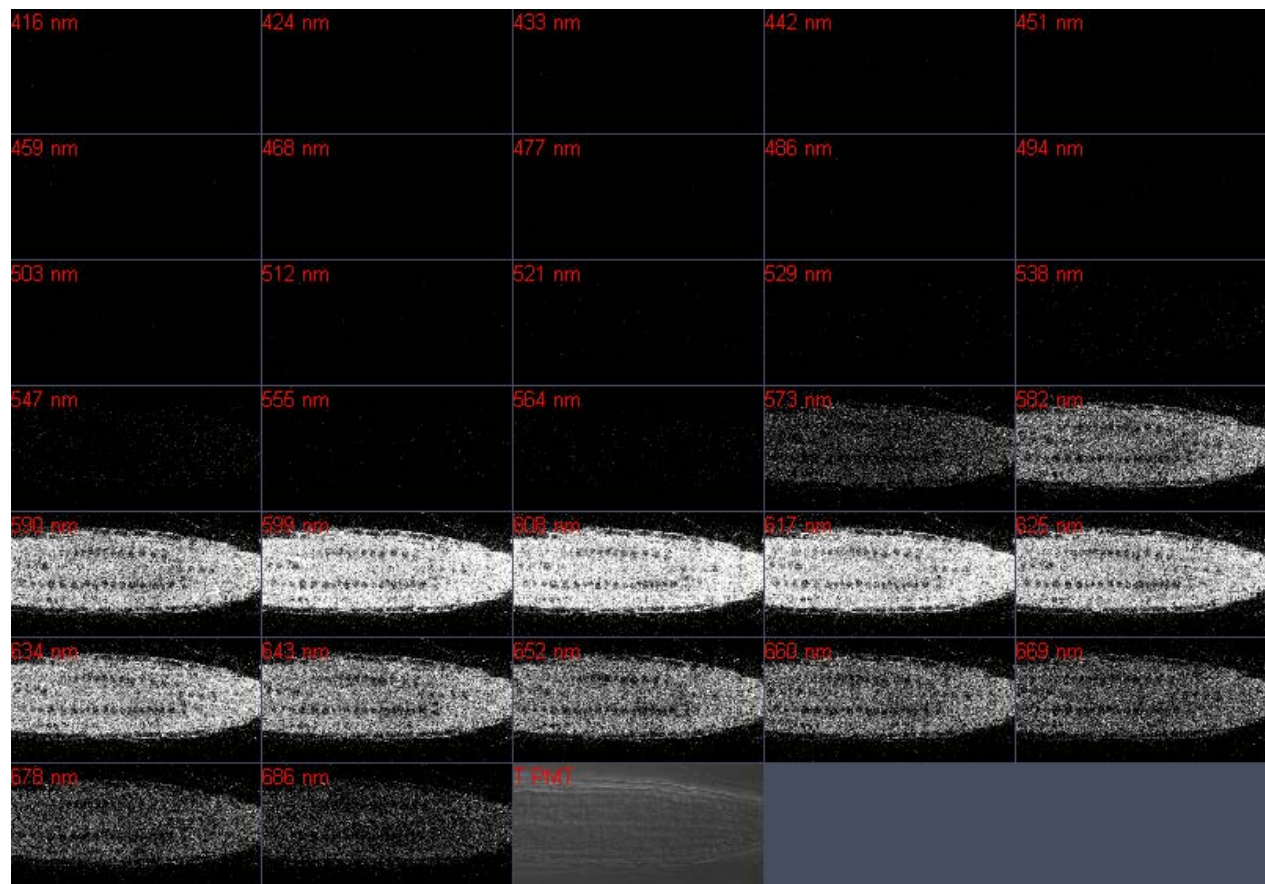


Figure 8.7: Lambda scan analysis in the epidermal layer of the root elongation and transition zone of five-day-old seedling of *aip1.2-1* mutant line complemented with functional *gAIP1-2-mCherry* (*aip1.2-1;gAIP1-2-mCherry*). Pictures were acquired using the 561 nm laser for excitation and the emission harvested in spectral intervals of 8-9 nm ranging from 416 to 686 nm wavelength. The last picture (T PMT) shows a transmission image.

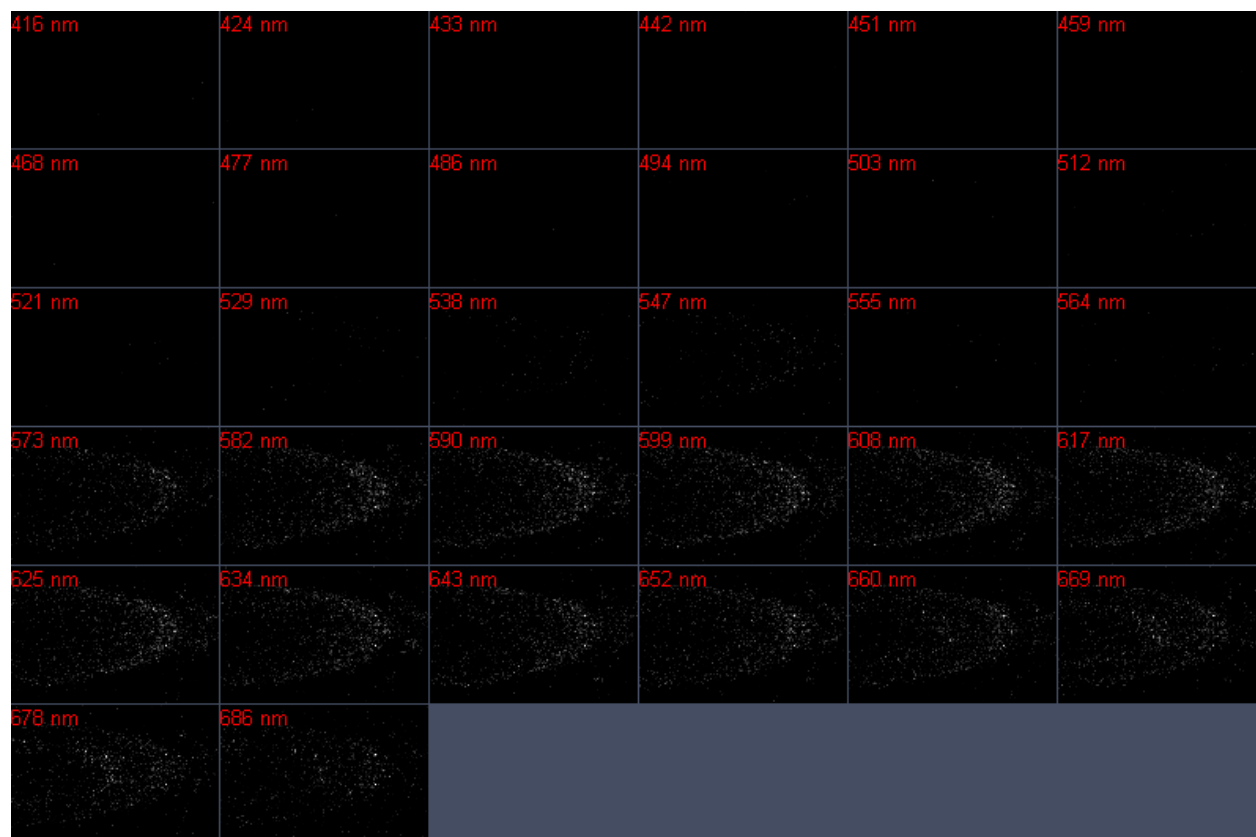


Figure 8.8: Lambda scan analysis in the epidermal layer of the root meristematic zone of five-day-old seedling expressing an ER-resident mCherry construct under control of the native *AIP1-2* genomic. Pictures were acquired using the 561 nm laser for excitation and the emission harvested in spectral intervals of 8-9 nm ranging from 416 to 686 nm wavelength.

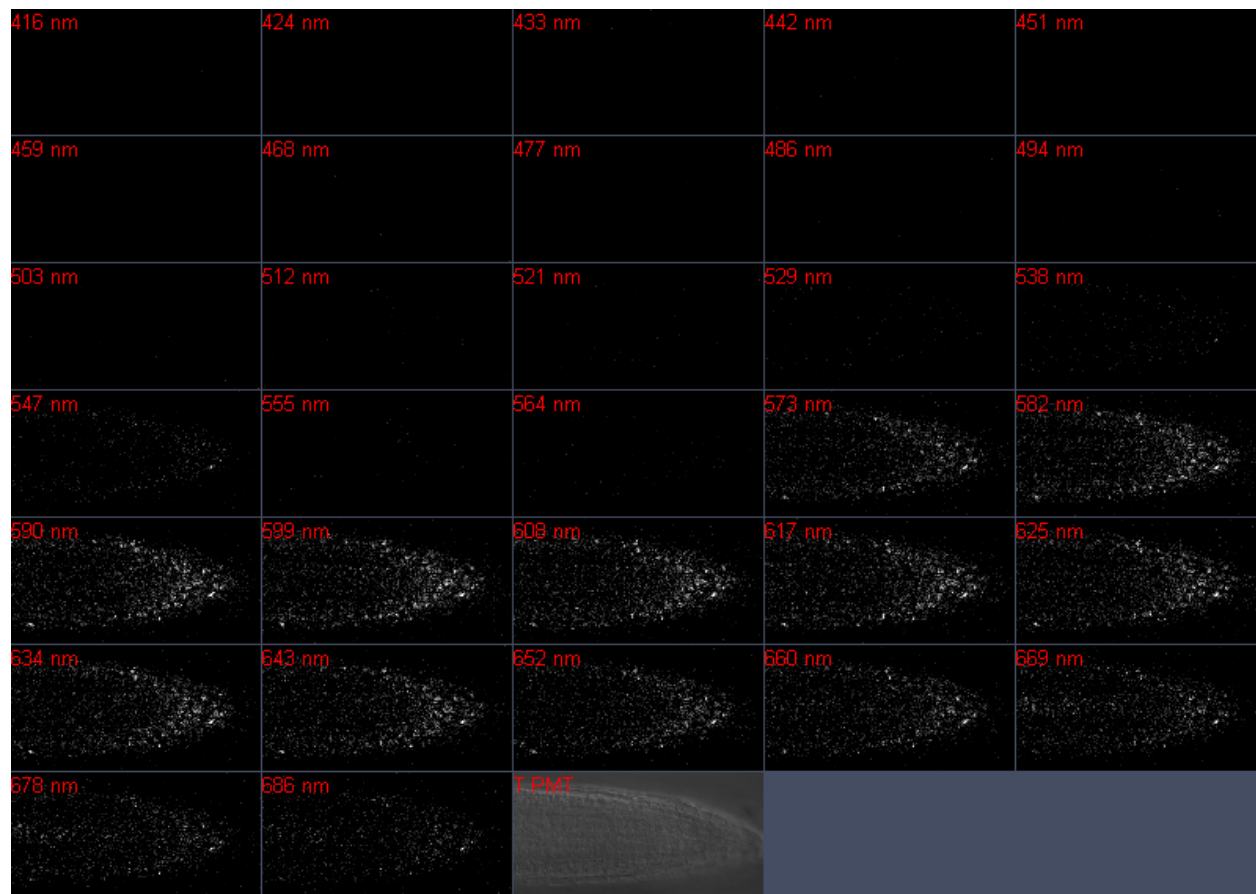


Figure 8.9: Lambda scan analysis in the epidermal layer of the root meristematic zone of five-day-old Col-0 wild type seedling. Pictures were acquired using the 561 nm laser for excitation and the emission harvested in spectral intervals of 8-9 nm ranging from 416 to 686 nm wavelength. The last picture (T PMT) shows a transmission image.

9. List of abbreviations

<i>A. thaliana</i>	<i>Arabidopsis thaliana</i>
ACT	actin
ADF	actin-depolymerizing factor
ADP	adenosine diphosphate
AIP1	actin-interacting protein 1
Arp2/3	actin-related protein 2/3 complex
ATP	adenosine triphosphate
<i>aux1</i>	<i>auxin resistant 1</i>
bp	base pairs
BSA	bovine serum albumin
CCD	charge-coupled device
CLSM	confocal laser scanning microscopy
Col-0	columbia-0
DNA	deoxyribonucleic acid
dNTP	deoxyribonucleotide
<i>E. coli</i>	<i>Escherichia coli</i>
ER	endoplasmic reticulum
ECL	enhanced chemiluminescence
<i>ein2</i>	ethylene insensitive 2
eYFP	enhanced yellow fluorescent protein
GFP	green fluorescent protein
<i>GL2</i>	<i>GLABRA2</i>
GST	glutathione S-transferase

His	Histidine
h	hours
IPTG	Isopropyl β -D-1-thiogalactopyranoside
<i>lacZ</i>	bacterial β -galactosidase gene
LB	lysogeny broth
min	minutes
NiNTA	nickel nitrilotriacetic acid
<i>MS</i>	Murashige and Skoog
<i>MSAR</i>	Murashige and Skoog for Arabidopsis
OD	optical density
PAGE	polyacrylamide gel electrophoresis
PCR	polymerase chain reaction
<i>PIN</i>	<i>PIN-FORMED</i>
PVDF	polyvinylidene fluoride
<i>RFP</i>	red fluorescence protein
RNA	ribonucleic acid
RNAi	RNA interference
<i>ROP</i>	Rho-of plants
rpm	revolutions per minute
s	seconds
SDS	sodium dodecyl sulfate
T-DNA	transfer DNA
TAE	Tris-acetate-EDTA
Taq	<i>Thermus aquaticus</i>
TBS	Tris-buffered saline

TBST Tris-buffered saline Tween-20

TEMED tetramethylenediamine

WER *WEREWOLF*